Response to reviewers and editorial comments on "New-gravity derived bathymetry for the Thwaites, Crosson and Dotson ice shelves reveals two ice shelf populations".

Reviewers comments in black, author responses in blue.

Reviewer 1:

Summary: The ice shelves play an important role in the stability of ice sheets through their buttressing effect. However, direct measurements could be difficult from different aspects, it is urgent to know what is happening underneath the ice shelves. So here, the authors present the improved topographic estimate underneath the Thwaites, Crosson and Dotson ice shelves (or the sub-ice-shelf cavity thickness) to help us how the warm ocean water access and interact with the glaciers' grounding lines.

Overall, I have several questions about this manuscript:
1. According to Section2.2, the author mentioned they used a similar method in An et al., 2019, which refers here as the topographic shift method. Both of these techniques could take the variations in crustal thickness, sedimentary basins or intrusions into account, so is there a conclusion to identify which method is better and why you choose the topographic shift method?

2. For Figure3, are the profiles across ice shelves, I am not sure this comparison makes sense. If I understand the material right, if the topographic shift method is constrained by Radar and swath observations, why the gravity shift method is not? In my opinion, both of these two methods should constrain by observations and inverted any other places where we don't have a direct measurement.

Minor: Text: Line237: typo Line250: format

We thank reviewer 1 for their comments on our manuscript. Our response to the key points raised is below:

1. We do not think that either the topographic shift or gravity shift method of An et al is intrinsically better. Both use topographic observations to constrain the final gravity derived topography, and both use interpolation of the error field between the known topographic points to generate an optimum correction. The use of constraining data to remove long wavelength trends induced by regional geology is the key point about both these methods, and where they are an improvement on the earlier method in this area which used a single DC shift. Our choice of the topographic shift method was simply driven by easy access to software.

2. Both the gravity shift method implemented in BedMachine (following the method of An et al) and the topography shift method we apply are constrained by observational data. However, the topographic shift approach is constrained by additional new swath and radar data collected for ITGC. The gravity shift method as implemented in BedMachine used the same, but more limited, input data as the older Millan 2017 method. This allowed us to show the key improvement from having a regionally varying correction, rather than the simple DC shift method. The topographic shift method we apply also excludes sub-ice shelf pinning points, which in some places appear to give rise to artefacts evident as topography where there is no gravity signal (Fig. 3d).

Referee #2

This paper presents new data and analysis and updates the sub-ice shelf bathymetry models of three major outlets of the West Antarctic Ice Sheet. As a technique paper this contribution is nice as it builds on previous

work well and is convincing that the perhaps incremental improvements made here are worthwhile to do in bathymetry inversions.
That being said, the discussion of error budget is lacking and while effort was made to compare the inversion to realistic observations to obtain a realistic error, this was only done in one relatively small area which I find inadequate for a general comment on uncertainty, especially considering the value is substantially lower than other similar work. The authors do a good job arguing that the basic bathymetry results should be an improvement over previous inversions of this area so it will be important for these maps to be available for ongoing numerical ocean modeling work. However, I believe the release of the bathymetry to the modeling community is the main contribution of this paper; in its current form the scientific discussion reads rather speculatively with a somewhat awkward discussion of grounding line retreat that I find largely unnecessary.

We thank reviewer 2 for their comments and provide a detailed response on a point by point basis below.

Specific comments:
Lines 54 to 56: The sentence referencing the Parker-Oldenburg method is misleading as it suggests that the problems discovered by the Cochran and Bell 2012 analysis that led to large disagreements between actual and inverted seafloor depth discussed in Brisbourne et al, 2014 were due to the algorithm used. The Parker-Oldenburg algorithm was never said to be the problem as there are many other more likely factors that may have contributed to the disagreement including platform speed, line-spacing/data coverage and resulting grid resolution, and, most importantly, the lack of explicit constraints on the geological forward model. To avoid misleading the readers, remove this discussion or replace with a full discussion of contributing factors, room permitting.

We agree that the Parker-Oldenburg algorithm was never considered the problem. We will therefore re-worded this section to clarify the fact that the problem lies in transformation of gravity signals directly into equivalent topography, and that such errors in the Larsen case-study were most likely to be due to the lack of explicit constraints on the underlying geology.

An overview of previous methods is an important introduction to our paper. We have therefore feel this section should be retained.

The additional point on the impact of data resolution, a function of platform speed, line spacing, data coverage and altitude is correct. We add the following text later in the manuscript:
"In addition to quantifying the errors it is important to note that the resolution of the bathymetry recovered from gravity data is limited by the wavelengths resolved by the gravity systems and the survey line spacing. For this study the gravity systems resolved minimum wavelengths of 5 to 10 km and a minimum line spacing of ~5 km is achieved outboard of Thwaites Glacier, while a minimum line spacing of ~7.5 km was achieved over the Dotson and Crosson Ice Shelves. This study therefore only recovered bathymetric features with a wavelength of ~5 km and upwards".

Line 92: The comparison in wavelengths between OIB and ITGC suggests an instrumentation difference; to clear this up please explain the improvement in resolution between the two campaigns –flight speed, elevation, instrumentation, etc.

The reviewer is correct, the OIB and ITGC use different platforms and gravity instruments and this will be clarified in an updated version of the text. We note that the ITGC data was collected on a twin otter platform which flies approximately half the speed of the OIB aircraft, so resolution of shorter wavelengths may be expected.

Line 95: Please explain what you mean by ""will have little impact". If you mean that not upward continuing to a common elevation could introduce errors when you invert a gravity gridded field that assumes a common

elevation then please state this is what you did. Although it seems right that +-200m will have little impact, please add an estimate of the error introduced. Please also include an estimate of the error introduced for the 5% of the lines flown higher than 450 m and lower than 1500 m and refer to a map in the Supplement illustrating that those lines (or line segments) are not in areas where those introduced errors will impact your interpretations/results.

By little impact we mean that continuation by +/- 200 m will change the peak amplitude of the observed gravity anomalies by up to ~+/-1 mGal. This would equate to ~+/- 14 m. variation in bathymetry which is well below any reasonable error for the recovered bathymetry. This point will be amended in any revised text.

A supplementary figure showing the range to ground on all gravity flight lines will be added to the text (and at the end of this document). It is apparent that one flight outboard from Thwaites glacier is flown ~200 m lower than the others. This may add a little extra resolution to the recovered bathymetry, but as noted above, not much. Over the Dotson/Crosson system there is one section of an OIB flight which is notably higher. This may bias the recovered bathymetry to be smoother than it really is, however, as noted in the text, downward continuation of this line would potentially introduce errors resulting from continuation procedure. We also note that if these line sections were contributing appreciable anomalous high or low frequency signals they would be apparent in the hill-shaded free air gravity anomaly field (Fig. 1c), which they are not.

Line 100: What is the stated resolution and uncertainty of the GOCO3 gravity model?
Please explain why the 2 mGal difference you observe more likely to be due to drift in the marine system rather than a regional variation not captured in the GOCO3 model.

The GOCO3 field is accurate to degree and order 250 (~160 km). We can-not rule out shorter wavelength geoid variability, or alternatively, that ice mass loss, coupled with GIA has locally altered the Geoid-Ellipsoid separation accounting for the residual 2 mGal error. The text will be updated on this point. However, we note that none of these issues will impact on recovery of the local bathymetry.

Line 181: Your error discussion currently highlights the 23 m contribution from crossover analysis and lack of geological knowledge. However, you have left out estimation of uncertainty due to platform speed, line spacing, and upward continuation. Either expand the discussion to including all sources of error in the budget or focus on the comparison with known bathymetry as you do later.

We believe the point the reviewer is making here relates to the intrinsic issue of the limited resolution of gravity derived bathymetry, which are a function of platform performance, speed, line spacing and flight elevation. This point on resolution is addressed above.

Line 200: Although I like your error estimation approach (comparing to known bathymetry), I don't think it is adequate to base your error for the whole survey region on only the multibeam area without at least showing that the errors are similar elsewhere; the multibeam area is less than 10% of your rather large survey area. This is additionally suspect as your 100 m error estimate is low compared to multiple other studies that quoted errors based on comparison with realistic bed data. This improvement in standard deviation is not expected considering that you are combining data from different platforms and instruments and your line spacing is coarse in many areas. Please present histograms for other areas to illustrate that both your mean and standard deviations are consistent where it matters –e.g. upstream of each grounding line. It may be helpful to compare your comparisons with known bathymetry to other studies that did something similar; the studies I'm aware of that also did this are: Brisbourne et al. 2014 (+-162 m), Greenbaum et al., 2015 (+-190 m), Hodgson et al. 2019 (+-175 m).

As noted in the text deriving error estimates for gravity derived bathymetry is challenging. If we had observations to do the error analysis we wouldn't need to do the inversion.

On the specific suggestion to perform similar analysis (exclude observational data – re-compute – and generate new error histograms) upstream of the Thwaites grounding line. This region unfortunately contains a significant geological structure which biases the gravity field. Any error estimate using the above approach would therefore suggest an error of several hundred meters, which the swath comparison suggests is not representative of the wider survey. We can-not categorically rule out the presence of similar geological bodies elsewhere in the survey area, however, the onshore structure has a distinct correlated high amplitude magnetic signature (Fig. 3b), which we do not see elsewhere beneath the ice shelves. The submarine environment that was used for the uncertainty comparison is also likely more representative of the submarine environment of the rest of the survey region than comparison with subglacial or subaerial exposed topography.

We note that an error of +- 100 m is not unreasonably low. For example An et al., 2019 estimated the error of the analogous gravity shift method to be ~60 m along the Greenland margin, while Tinto et al reported an estimated error of ~68 m for the Ross Ice Shelf area, excluding sensitivity to unconstrained geological variations. It is un-surprising that the Larsen Ice shelf gave higher errors, as no robust account was made for the geology of the region. In the case of the Hodgson et al. 2019 paper the 175 m error was before adjustment to the controlling seismic, swath and radar data, and should be considered a worst-case error for an unconstrained inversion of gravity data. The true error in that study will by definition be less than the suggested 175 m. Hodgson et al. 2019 suggest an error estimate of ~100 m is appropriate, based on how accurately the gravity derived bathymetry predicts ice shelf grounding depths.

Line 206: Typo: remove "there" after "where"
Amended
Line 248: Please replace "typical shelf water" with something more descriptive.
Re-written.

Line 255: Please revise this sentence regarding MCDW supply. The supply of MCDW should be limited more by the depth of the shallowest bathymetry between source of the MCDW and the grounding line, not by the thickness of the water column near the grounding line. Profile C indicates a relatively shallow (500 m) sill which could reduce the supply of MCDW depending on the average thermocline depth which you refer to as 400-600 m. Unless you meant something else by "limit the supply of mCDW". Later on line 319 you connect weak circulation with thin cavities, is that what you mean by TCD limit the supply? If so, please connect this thought in both places.

We acknowledge that shallow bathymetry is the most obvious limit mCDW flow, however, in this case it is the cavity thickness that we suggest could limit flow. We will make this point more explicitly in the revised text and, as suggested, will better link this sentence to the part later in the paper.

Line 273-274: Your comment connecting the slight positive correlation to MCDW being forced onto shallow topography is very speculative and perhaps unnecessary; I recommend removing it otherwise please list other explanations for the correlation.

OK we have removed this speculation.

Line 320 to 330: It strikes me as an intuitive and even mundane result that more recently ungrounded ice shelf areas would have a tighter correlation with bathymetry than ice shelf areas that ungrounded previously. The discussion of this as it stands does not provide enough additional insight to convince me that the older shelf areas don't simply lose the correlation because they've just had more time to spread under their own weight and

melt. It is also expected that recently ungrounded areas are the most likely to re-ground under a new flow regime or ocean conditions. I concede that I may have missed a subtle (or not so subtle) nuance, if so, please revise this discussion in a concise manner in your response otherwise I recommend shortening this section and moving the correlation plots to the supplement.

We acknowledge that this section was overly complicated and will shorten it to make it more concise (Including removing Figure 6). However, while we agree that the observation of thin new sub-shelf cavities may be intuitive, we do not believe it is mundane for two reasons.

1: The very large areas (>30 km wide) covered by thin cavities indicate that extremely high melt rates required to drive retreat are focused at the grounding line, and not a widely dispersed phenomenon. This is a result which must be predicted by any future model of ice shelf evolution.

2: The basal profile of an ice shelf in dynamic equilibrium with the ocean in this region would rise steeply seaward of the grounding line and continue rising at least until it reaches the mCDW thermocline depth. We show that this is not the case for the recently evolved ice shelves, hence using a simple equilibrium model would miss important details of the system evolution.

Figure 6 seems unnecessary when you can refer to the literature for this information. I recommend either moving it to the supplement or at least stacking them vertically and placing them next to the thinning map in Figure 7 to save space.

Figure will be removed

References: Please add standard indentation to improve readability for the next revision.

Format will be updated.

Editor's note:

Dear Dr. Jordan et al.,

I've read through your initial submission and consider it suitable to send out to review. However, if the referees don't bring it up, I will strongly recommend the following:

- While published only recently, the authors are certainly aware of BedMachine Antarctica (Morlighem et al, 2019, Nature Geoscience), which is a significant advance over Bedmap2. The manuscript as it stands is immediately dated by a comparison with Bedmap2 in Figure 1, and some of the discussion of the differences with Milan et al. (2017) partly stems from their use of MC onshore, which I assume was also incorporated in Morlighem et al. (2019). I encourage the authors to switch over to using BedMachine Antarctica absent a contraindicating argument, which will extend the shelf life of this manuscript.

We recognise that BedMachine Antarctica was a significant advance on Bedmap2 in many respects. BedMachine Antarctica included bathymetry derived using the gravity shift method. We will therefore replaced our comparisons between the gravity shift results with comparisons to BedMachine Antarctica (see supplementary figure 2 below).

However, we note that the mass conservation approach does make assumptions and can change 'real' topography observed by radar. By constraining our recovered bathymetry only with observed radar derived topography, or swath bathymetry, we ensure our inversion is independent of as many additional assumptions as possible. Given the very good radar coverage in the Thwaites glacier region the use of mass conservation rather

than the 'real' data should have relatively little impact. It is interesting to note that BedMachine shows a consistent offset of ~34 m for the onshore part of the Thwaites catchment compared to our result which is derived simply from the radar bed pick and geoid correction. The origin of this offset is not clear to the authors, but further investigation of this on-shore observation is beyond the scope of this paper.

In addition our constraining compilation includes new radar and multibeam bathymetry data which were collected and processed after BedMachine Antarctica was produced. Although the new radar data is a relatively minor component, in regions such as Bear Island which were sparsely covered, they provide important constraints. By including these new data we ensure the best possible constraint on our predicted sub-ice shelf bathymetry.

- More exposition and emphasis on the two-population concept that you introduce in the title. Figure 5 is quite interesting and compelling support of the concept, but I found the two panels in Figure 6 difficult to distinguish from each other.

In line with your suggestion and that of reviewer 2 we have made the section on the two ice shelf populations more concise and removed Figure 6, as we did not feel it added enough to the discussion.

- In several figures, reconsider the green-to-red grounding-line history overlain on green-to-red topography.

We have amended the colour-scales of the underlying datasets on these figures so that the grounding-lines stand out more clearly.

Thanks for submitting your work to The Cryosphere,

Joe MacGregor
NASA/GSFC

New gravity-derived bathymetry for the Thwaites, Crosson and Dotson ice shelves revealing two ice shelf populations

Tom A. Jordan[1], David Porter[2], Kirsty Tinto[2], Romain Millan[3], Atsuhiro Muto[4], Kelly Hogan[1], Robert D. Larter[1], Alastair G.C. Graham[5], John D. Paden[6]

[1] British Antarctic Survey, High Cross, Madingley Road, Cambridge, CB3 0ET, UK
[2] Lamont Doherty Earth Observatory
[3] Institut des Géosciences de l'Environnement, Université Grenoble Alpes, CNRS, 38000 Grenoble, France
[4] Dept. of Earth and Environmental Science, Temple University, Philadelphia, PA 19122, USA
[5] College of Marine Science, University of South Florida, St Petersburg, FL 33701, USA.
[6] Center for Remote Sensing of Ice Sheets (CReSIS), The University of Kansas, Kansas 66045, USA

Correspondence to: Tom A. Jordan (tomj@bas.ac.uk)

Abstract. Ice shelves play a critical role in the long-term stability of ice sheets through their buttressing effect. The underlying bathymetry and cavity thickness are key inputs for modelling future ice sheet evolution. However, direct observation of sub-ice shelf bathymetry is time consuming, logistically risky, and in some areas simply not possible. Here we use new compilations of ~~airborne gravity anomaly~~airborne and marine gravity, radar depth sounding and swath bathymetry ~~data~~ to provide new estimates of sub-ice shelf bathymetry outboard of the rapidly changing West Antarctic Thwaites Glacier, and beneath the adjacent Dotson and Crosson Ice Shelves. This region is of especial interest as the low-lying inland reverse slope of the Thwaites glacier system makes it vulnerable to marine ice sheet instability, with rapid grounding-line retreat observed since 1993 suggesting this process may be underway. Our results confirm a major marine channel >800 m deep extends to the front of Thwaites Glacier, while the adjacent ice shelves are underlain by more complex bathymetry. Comparison of our new bathymetry with ice shelf draft reveals that ice shelves formed since 1993 comprise a distinct population where the draft conforms closely to the underlying bathymetry, unlike the older ice shelves which show a more uniform depth of the ice base. This indicates that despite rapid basal melting in some areas, these "new" ice shelves are not yet in dynamic equilibrium with their retreated grounding line positions and the underlying ocean system, a factor which must be included in future models of this regions evolution. ~~We propose qualitative models of how this transient ice shelf configuration may have developed.~~

1 Introduction

The Thwaites Glacier system is a globally important region of change in the cryosphere system (Fig. 1a) (Scambos et al., 2017). In this region the marine based West Antarctic Ice Sheet comes into direct contact with upwelling modified Circumpolar Deep Water (mCDW) which is warm relative to the typical cool dense shelf water on Antarctic continental shelves (Jenkins et al., 2018). This warm water can both erode the buttressing ice shelves, and directly melt the grounded ice, both factors driving dynamic thinning and retreat of glaciers and contributing to rising global sea level (Pritchard et al., 2012). The inland reverse

slope of the bed beneath Thwaites Glacier and some of the adjacent glaciers means that marine ice sheet instability may occur (Schoof, 2007;Weertman, 1974). In this case a feedback is setup where grounding line retreat exposes a progressively larger cross-sectional area of ice, hence more ice fluxes into the ocean leading to further glacial retreat. Satellite observations revealing an increase in the velocity of ~100 ma^{-1} extending ~100 km inland from the Thwaites grounding line and surface draw down of over 1 ma^{-1} indicate that this region is changing now (Gardner et al., 2018;Milillo et al., 2019). It has been argued that dramatic retreat of the grounding lines of Thwaites, Pope, Smith and Kohler glaciers of between 10 and 30 km since 1993 (Fig. 1a) means that ice sheet collapse due to marine ice sheet instability may have begun (Rignot et al., 2014;Milillo et al., 2019;Joughin et al., 2014).

Understanding the ~~sub-ice-shelf~~ bathymetry beneath the ice shelves separating the open marine realm of the Amundsen Sea Embayment and the grounded ice of the Thwaites Glacier system is of particular importance for the evolution of this region (Fig. 1a). The bathymetry beneath ice shelves is a fundamental control on the ice sheet stability as the shape of the water cavity is a first order control on sub-ice shelf currents, including the flux of warm, deep ocean water to the ice shelf bases and the grounding line beyond (Jacobs et al., 2011). Melting, thinning and ultimately disintegration of ice shelves will trigger faster glacial flow, forcing glacial retreat, leading to global mean sea level rise (Scambos et al., 2004;Rignot et al., 2014). Cavity shape is also likely an important factor controlling the rate of melting close to the grounding line (Milillo et al., 2019;Schoof, 2007). Direct measurements of sub-ice-shelf bathymetry by seismic ~~spot measurements~~sounding is slow and often impractical due to the extremely crevassed environment (Brisbourne et al., 2014;Rosier et al., 2018). Exploration of sub-ice-shelf cavities using autonomous underwater vehicles can also be risky and time consuming to attain regional coverage (Jenkins et al., 2010;Davies et al., 2017). An alternative technique to provide a first-order estimate of the bathymetry is the inversion of airborne gravity anomaly data, which can be collected quickly and efficiently over large areas.

Recovery of bathymetry from gravity data relies on the fundamental fact that the density contrast at the sea bed gives rise to significant and measurable gravity anomalies. A variety of techniques have been employed to invert gravity data for bathymetry. In the simplest case, the free-air anomaly is transformed directly to an equivalent ~~bathymetric~~ surface assumed to reflect the bathymetry. This can be done ~~, typically~~ in 3D using a fast Fourier transform approach such as the Parker–Oldenburg iterative method (Gómez-Ortiz and Agarwal, 2005), as applied to the Larsen Ice Shelf (Cochran and Bell, 2012). ~~However, subsequent seismic observations indicate that, a~~Although the broad pattern of the bathymetry is~~was~~ resolved, ~~this approach~~transformation of gravity signals directly into equivalent topography can give rise to significant errors, attributed in the case of the Larsen Ice Shelf to geological factors such as crustal thickness and sedimentary basins distorting the gravity field (Brisbourne et al., 2014). An alternative technique models the bathymetry using gravity data along multiple 2D profiles, for example across the Abbot Ice Shelf (Cochran et al., 2014) and outboard of Thwaites Glacier (Tinto and Bell, 2011;Tinto et al., 2011). Such models are constrained to match known topography and inferences about the underlying geology provide additional constraints. The 3D bathymetry beneath the Pine Island Glacier ice shelf was inverted from gravity data using a 3D prism model and a simulated annealing technique solving for bathymetry and a sedimentary layer (Muto et al., 2016). Although this technique returns a bathymetry model constrained by observations, it is not clear whether signatures due to sediments and

bathymetry can be reliably separated without *a priori* constraints such as seismic observations (Roy et al., 2005). More recently, a 3D model constrained by regional bathymetry and subglacial topography was used to model bathymetry offshore of Pine Island and Thwaites glaciers, and beneath the Crosson and Dotson Ice Shelves (Millan et al., 2017). This model showed a complex topography with deep channels extending to the margin of the ice sheet, particularly in the Dotson-Crosson area where previously-unknown deep (>1200 m) channels were identified.

In this paper we re-evaluate the sub-ice-shelf bathymetry offshore from Thwaites Glacier and beneath the Crosson and Dotson Ice Shelves (Fig. 1a) through the integration of new airborne gravity data collected during the 2018/19 field season as part of ~~from~~ the NERC/NSF International Thwaites Glacier Collaboration (ITGC), Operation IceBridge (OIB) (Cochran and Bell, 2010, updated 2018) and new marine gravity data from the R/V Nathaniel B. Palmer collected during the cruise NBP19-02 (Fig. 1b). To recover bathymetry from gravity beneath the ice shelves we employ an algorithm-based approach similar to that used for the Brunt Ice Shelf (Hodgson et al., 2019). This approach constrains the recovered topography to match all direct topographic observations. This constraint helps account for geological factors such as variations in crustal thickness, sedimentary basins, or intrusions. We acknowledge that away from direct topographic observations the uncertainties in the bathymetric estimate due to geological factors increase. However, we suggest that using a well-constructed gravity-derived bathymetry is preferable to unconstrained interpolation across sub-ice-shelf bathymetric data gaps many 10s of kilometres wide. Such use of gravity data is routine for predicting topography in un-surveyed parts of the ocean using satellite data (Smith and Sandwell, 1994) and is being used in the Arctic where higher resolution airborne data are included (Abulaitijiang et al., 2019).

Our results confirm the shape and position of the previously identified troughs (Millan et al., 2017). Differences in the inversion results beneath the inboard parts of some of the ice shelves are identified, reflecting the higher resolution of the new gravity data set and differences in the methods used. Our improved topographic estimate reveals variations in sub-ice-shelf cavity thickness, which have implications for the rate at which the warm ocean water can access the present-day grounding lines, and the mechanism of grounding line retreat in these and other areas.

2 Methods

2.1 The integrated gravity and topographic data sets

We utilise airborne gravity data from OIB and the ITGC campaign, together with marine gravity data from cruise NBP19-02 (Fig. 1b and c). The OIB free-air gravity data were collected from a DC-8 aircraft travelling at ~120 ms^{-1} at an altitude of ~450 m above the ice surface, using the Sander Geophysics AirGrav system (Studinger et al., 2008). These data have~~s~~ an error of ~1.67 mGal in this region and resolve~~s~~ anomalies with a ~10 km full wavelength (Cochran and Bell, 2010, updated 2018;Tinto and Bell, 2011). The ITGC campaign utilised a different 'strapdown' gravity approach based around an iMar Inertial Navigation System (INS) (Becker et al., 2015;Wei and Schwarz, 1998), resulting in data with an internal error from crossover analysis of 1.56 mGal and resolving wavelengths down to ~5 km (Jordan et al., 2020c) (see supplementary data Section S2 for

details). Airborne data were restricted to lines flown at <1500 m above the surface. Of this subset over 95% of the data were collected at 450 m ±200 m above the surface. Upward and downward continuation of the gravity data to a common altitude was neglected as continuation by ~200 m will have little impact on the amplitude of the gravity anomalies (~1 mGal) given the ~1000 m range to the key bathymetric sources. Downward continuation can also introduce unnecessary artefacts and neglecting upward continuation preserves short wavelength gravity information. The data collected >650 m from the ice surface may give rise to an artificially smooth bathymetry, but are spatially restricted (SFig. 1), and do not appear to give rise to any anomalous signals in the integrated free air gravity dataset (Fig. 1c). Marine gravity data from cruise NBP19-02 matched the pattern of the airborne anomalies, but ~~was~~ were offset by ~7.14 mGal above the level of the airborne data. The majority of this offset is due to the difference between geoid (marine) and ellipsoid (airborne) references used for the different systems. In the area of overlap the geoid-ellipsoid difference results in a ~9 mGal discrepancy, based on the GOCO3s satellite gravity model (Pail et al., 2010). The residual ~ 2 mGal difference may reflect drift in the marine system, and potential discrepancies in base station ties between the different surveys. Alternatively un-considered shorter wavelength variability in the gravity field not resolved by the GOCO3s model (<~160 km), or temporal changes in the geoid associated with glacio-isostatic adjustment and mass loss may account for the residual shift. Such features do not impact the locally recovered bathymetry ~~The~~ and are beyond the scope of this paper. The average measured shift of 7.14 mGal was therefore ~~removed~~ subtracted from the marine line data as a single DC value ~~as the variation in geoid-ellipsoid discrepancy in the overlap area is <0.1 mGal~~. All line data were then merged into a single database, interpolated onto a 1 km mesh raster and filtered with a 5 km low pass filter removing residual line to line noise. This filter wavelength is justified as anomalies with wavelengths <5 km are not ~~expected to be~~ resolved by the airborne gravity systems used. The final, integrated free-air gravity map (Fig. 1c) shows a clear pattern of high and low anomalies, which to first order match the main 5-10 km wavelength features visible in the available onshore subglacial topography and offshore bathymetry (Fig. 1d).

The topographic observations onshore were taken from OIB line radar data (Paden et al., 2010, updated 2018), augmented with new depth sounding radar collected along with the gravity data during the ITGC campaign (Fig. 1d). This new bed elevation data was collected using a ~~550~~600-900 MHz accumulation radar provided by the Center for Remote Sensing of Ice Sheets (CReSIS). Bed elevations were picked from SAR processed radargrams in a semi-automated fashion. Although the primary target of this radar system was shallow ice sheet structures bed elevation was resolved through ice up to ~1900 m thick. Visual inspection revealed a few incorrect onshore bed picks in the OIB dataset on Bear Island, which gave bed elevations above the highly accurate REMA surface digital elevation model (DEM) (Howat et al., 2019). These points were deleted from the integrated line bed elevation dataset. The line bed elevation data were corrected to the GL04c Geoid (Forste et al., 2008), and the data interpolated onto a 1 km mesh raster. This gridded dataset was carefully masked to remove regions which are now covered by the floating ice shelf based on the most up to date grounding lines (Rignot et al., 2014;Milillo et al., 2019). Bed elevation values over local sub-shelf pinning points were also excluded. This masking mitigates the risk of the base of a floating ice shelf being misidentified as a bed elevation point and biasing the inversion. Beyond the ice shelves we took

the values constrained by a new compilation of shipborne multibeam swath bathymetric data (Hogan et al., 2020), which was down sampled to a 1 km mesh raster for this study (Fig. 1d).

2.2 Recovering sub-ice-shelf bathymetry

To recover a gravity-enhanced bathymetry we follow an algorithmic approach, rather than a pure inversion (Hodgson et al., 2019). We refer to this as the *topographic shift* method, as an initial topographic estimate derived from the gravity data is shifted to match observed topographic tie points. Summarising the method, the initial 3D topographic estimate (SFig. 2a) was calculated from the free-air anomaly (Fig. 1c~~, and SFig. 1a~~) using an iterative forward modelling method (von Frese et al., 1981). Differences with between the initial topographic estimate (SFig. 2b), and the observed bathymetry and onshore topography were calculated (Fig. 1d~~, and) SFig. 1b),~~ and interpolated using a tensioned spline (Smith and Wessel, 1990).~~, and~~ This difference grid was then subtracted from the initial topographic estimate to provide the final bathymetric estimate (Fig. 2a). For full detail on the method see supplementary material Section S1. The topographic shift method is conceptually similar to the *gravity shift* method developed and applied along the Greenland coast where the initial free-air gravity data were shifted to match the variable gravity field from models of known topography prior to inversion for bathymetry (An et al., 2019). This gravity shift method was subsequently employed to fill the sub-ice shelf bathymetry in the Thwaites Glacier region of the recent BedMachine Antarctica compilation (SFig.5c) (Morlighem et al., 2020). The advantage of both ~~of these~~the topographic and gravity shift techniques is that features in the gravity field due to variations in crustal thickness, sedimentary basins or intrusions are implicitly taken into account, as long as they overlap with the topographic control points. This assumption is most robust for long wavelength features such as variations in crustal thickness, or regional sedimentary basins, where the associated errors will impact multiple topographic control points allowing good control of the resulting error field. The impact of more localised geological features which only partially overlap constraining topographic data will be less well defined and we make the assumption that such errors fall off smoothly away from the affected control points. Geological features which have no overlap with constraining topographic observations can still introduce artefacts distorting the recovered bathymetry in proportion to their size and density contrast.

2.3 Ice shelf draft and cavity thickness

The depth of the ice shelf base, and the thickness of the sub-ice-shelf water filled cavity (Fig. 2b) were calculated assuming the ice shelf is in hydrostatic balance (Griggs and Bamber, 2011). Hydrostatically defined draft is typically a good approximation to radar measured ice thickness (Griggs and Bamber, 2011) and provides seamless coverage of our study area. The input surface elevation data were taken from the REMA digital elevation model (DEM) (Howat et al., 2019) corrected to the GL04c Geoid (Forste et al., 2008). In the study area the REMA DEM is based on satellite observations between 2014 and 2016, and therefore reflects the surface elevation after widespread un-grounding between 1993 and 2014 (Rignot et al., 2014). Ice and water densities were assumed to be 917 and 1027 kg m^{-3}, respectively, and a 16 m firn correction was applied (Griggs

and Bamber, 2011). Uncertainties in these assumed values may have an impact on the precise values of ice shelf draft, but are unlikely to significantly distort the calculated pattern of water cavity thickness. Errors in ice shelf draft of up to 80 m in the 10-25 km most proximal to the grounding line may occur due to the rigidity of the ice shelf (Rignot et al., 2011), but in Thwaites glacier this 'bending zone' appears to be narrow (<5 km) (Milillo et al., 2019), which we attribute to the highly fractured nature of the ice shelf in this region.

3 Results

Our modelled sub-ice-shelf bathymetry (Fig. 2a) reveals a complex offshore topography from ~250 to >1000 m deep, with a pattern of ridges and troughs of a size and scale consistent with the terrain mapped onshore with radar, and offshore with multi-beam swath bathymetry. All the key bathymetric features we observe are imaged as anomalies in the free-air gravity data, and are therefore not artefacts of the inversion technique. Many of the isolated pinning points seaward of Thwaites Glacier and beneath the Crosson Ice Shelf shown by InSAR-derived grounding lines (Rignot et al., 2014) are revealed by our study as being ~~underlain by~~situated on broader bathymetric highs. In these areas our recovered topography predicts that the ice shelf is grounded, or ~~be~~ within 100 m of grounding (i.e., the water column is calculated to be less than 100 m thick; Fig. 2b). As our inversion did not use any additional data (swath, seismic or radar) to constrain the elevation at these isolated pinning points within the ice shelves the fact that many appear to be within error of their grounding level provides qualitative support for the reliability of our inversion.

The revealed sub-ice-shelf cavity is >500 m thick in many areas. Adjacent to parts of Thwaites Glacier this deep cavity reaches to within 0-10 km of the grounding line. In contrast the inboard parts of the Dotson and Crosson Ice Shelves formed since 1993 overlie a cavity typically <150 m thick (Fig. 2b), and the thick (>450 m) cavity lies more than 10-30 km from the current grounding line.

Profiles of the bathymetry beneath the ice shelves confirm the complex sub-ice-shelf pattern (Fig. 3). Our results show that the tips of both the Eastern Ice Shelf and Thwaites Glacier Tongue are grounded at their seaward ends on a linear but dissected ridge, while a ~1000 m deep sub-ice-shelf cavity is apparent behind the pinning ridge (Figs. 3a and b). Where the grounding line of the Thwaites Glacier Tongue has retreated since 1993 the estimated ice shelf base closely follows the modelled bathymetry (Fig. 3b). Along the narrow channel close to Bear Island a cavity >500 m thick is apparent beneath the Crosson Ice Shelf, but this does not extend into the region where the grounding line has retreated most significantly in the recent decades (Khazendar et al., 2016) (Fig. 3c). Profiles across the Dotson Ice shelf towards Kohler Glacier indicate the grounding line is separated from the main sub-ice-shelf cavity by a sill, which appears to reach within ~200 m of the base of the ice shelf (Figs. 2b and 3d).

4 Discussion

4.1 Quantification of errors

Quantification of the errors associated with gravity inversions is challenging as a combination of intrinsic but quantifiable uncertainties in the gravity data, the inversion assumptions, and the poorly understood variability of sub-surface geology all contribute to the error budget. Errors in the gravity field of ~1.56 mGal defined from crossover analysis directly contribute to ~23 m uncertainty in the recovered bathymetry. The modelled rock density of 2670 kg m^{-3} assumes no sediments are present at the sea floor. This is reasonable given the generally rugged morphology observed across many parts of the Amundsen Sea inner shelf (Nitsche et al., 2013;Graham et al., 2009;Larter et al., 2009). However, assuming all bathymetry was carved into lithified sediment the total amplitude of the sub-ice-shelf topography could be underestimated by ~11% (~130 m), assuming a typical sediment density of 2500 kg m^{-3} (Telford et al., 1990). Lower density un-lithified sediment could lead to an even larger underestimates of topographic amplitude, but such material would not be expected to form all of the >1000 m high ridges recovered by our inversion and imaged by recent swath data (Hogan et al., 2020). Other geological factors such as dense gabbroic intrusions, or local sedimentary basins could further distort the recovered bathymetry if they are away from the direct bathymetric observations which would mitigate the impact of such features on the final bathymetric model. Underlying geological factors can, in some cases, be revealed by coincident aeromagnetic data, as in the case of the Brunt Ice Shelf (Jordan and Becker, 2018;Hodgson et al., 2019) and Ross Ice Shelf (Tinto et al., 2019). In our study, tight correlation between high amplitude magnetic (Jordan et al., 2020b) and gravity anomalies is only seen beneath the grounded part of Thwaites Glacier (Fig. 3b). Such tight correlation is indicative of a significant geological feature distorting the gravity signature (Jordan and Becker, 2018), but is not seen on profiles across the offshore regions (Fig. 3). This favours a model where underlying geological factors are not dominating the inversion results.

In addition to quantifying the errors it is important to note that the resolution of the bathymetry recovered from gravity data is limited by the wavelengths resolved by the gravity systems and the survey line spacing. For this study the gravity systems resolved minimum wavelengths of 5 to 10 km and a minimum line spacing of ~5 km is achieved outboard of Thwaites Glacier, while a minimum line spacing of ~7.5 km was achieved over the Dotson and Crosson Ice Shelves. This study therefore only recovers bathymetric features with a wavelength of ~5 km and upwards.

To best quantify the uncertainty in the sub-ice-shelf bathymetric estimate in our study region we utilised the new shipborne multibeam bathymetric data collected predominantly by a recent ITGC cruise, NBP19-02 (Fig. 1a) (Hogan et al., 2020). The topographic shift method was re-run with this multibeam data excluded from the constraining bathymetric dataset (Fig. 4a). The difference between the results with and without this test dataset (Figs. 4a and b) provides a snap-shot of the errors associated with our recovered bathymetry (Fig. 4c). In this region the mean error is -40 m, with a standard deviation of 100 m. We take this standard deviation to be representative of the expected error in our modelled bathymetry. This error is within the typical range for that quoted for gravity derived bathymetry, for example error estimates of ~60 m have been suggested in Greenland (An et al., 2019), while errors of up to ~160 m are suggested for the Larsen Ice Shelf where, unlike our study, no

account had been made for the underlying geology (Brisbourne et al., 2014;Cochran and Bell, 2012). The mean error we find indicates that the bathymetry constrained by the swath data is deeper than predicted by the gravity inversion alone, and hence that that there are geological features in this region distorting the recovered bathymetry. It is apparent that the largest errors are associated with higher frequency topography revealed by the new multibeam data. Such errors resulting from comparison of datasets with fundamentally different resolutions is to be expected, highlighting the need for multibeam bathymetry in regions where sub-kilometre-scale resolution of bathymetry is required. This is particularly relevant in areas where ~~there~~ the seabed topography includes high amplitude variations at short wavelengths. In addition, this pattern of errors means that single seismic observations of cavity depth may not be ideal tie points for gravity inversions in rugged regions such as near Thwaites Glacier. A single such seismic measurement typically relies on a receiver array ~250 m long (Brisbourne et al., 2014) and hence could image a local high or low, biasing the wider gravity inversion.

4.2 Previous bathymetric estimates

Comparison between our topographic shift method and previous gravity inversions in this region show the broad sub-ice-shelf features are resolved by all methods, but differences in the detailed results are clear (SFig. 5). The OIB Level 3 data product (Tinto et al., 2011;Tinto and Bell, 2011) shows the largest discrepancies (SFigs. 5a,d and Figs. 3a,b), with our new inversion showing bathymetry 200 to 300 m shallower at the grounding line. This in part reflects the fact that the OIB bathymetric estimate was limited to using 2011 and older gravity data. In addition this bathymetric model relied on integrating the results of a series of 2D forward gravity models, incorporating observed bathymetry and radar-derived topography ~~of~~ beneath the grounded ice. These gravity models did not factor in any regional trends in the gravity field, but rather corrected for a single DC shift at the outboard end of each profile, and modified the upper crustal density at the inland end of the profile to achieve a good fit. Un-modelled regional trends could, therefore, be a factor distorting the recovered bathymetry.

The Millan et al. (2017) inversion of bathymetry from gravity data shows the same general pattern of sub-ice-shelf bathymetry as our topographic shift method (SFig. 5b). However, differences are observed, most clearly beneath the inboard parts of the Dotson Ice Shelf (SFig. 3e). In addition significant undulation in the recovered bathymetry, not associated with any gravity signal are seen, for example from 100 to 120 km in Figure 3d. Such variability is indicative of artefacts due to the inversion approach. As our topographic shift method is different, and we incorporate additional new gravity, ~~and~~ bathymetric and radar data, it is not immediately clear what the source of these discrepancies are. To independently asses the results of Millan et al., (2017) we ~~calculate a revised bathymetry~~compare their results with BedMachine Antarctica (Morlighem et al., 2020) (SFig. 4c) ~~using~~ which used the same input data as Millan et al. (2017), and the gravity shift method previously applied to the Greenland margin (An et al., 2019). The key difference between the An et al., (2019) and Millan et al., (2017) methods is that the newer approach applies a variable rather than single DC shift to the gravity prior to inverting for the bathymetry~~, but in other respects the methods closely match~~. The residuals between the Millan et al., 2017 result and ~~the~~BedMachine Antarctica (the gravity shift method) (SFig. 4f) show~~s~~ a similar pattern to the residuals between the Millan et al., 2017 result and our

topographic shift method (SFig. 4e). This indicates that the use of a single DC shift was a significant issue in the older inversion (Millan et al., 2017) which may have led to an over-estimate of the depth of some near-shore features.

Comparing BedMachine Antarctica ~~the gravity shift~~ and our topographic shift results reveals that differences of over 250 m are still present (SFig. 5~~4~~g). We suggest that these remaining differences reflect the additional multibeam bathymetric, ITGC radar and gravity data used in our topographic shift result.~~,~~ In addition the different bed topography onshore (OIB and ITGC line radar data ~~flights~~ here vs. mass conservation in BedMachine Antarctica (Morlighem et al., 2020) ~~Millan et al., 2017)~~ and exclusion of sub-ice-shelf pinning points from ~~the~~ our topographic shift result also likely contributed to the differences. For example topography with no associated gravity signal is seen in the BedMachine profile in Fig. 3d, indicating the method and tie points used introduced some artefacts. This highlights the need for caution when using -gravity-derived bathymetry and the value of high resolution gravity data with tight line spacing such as the integrated OIB/ITGC dataset, together with additional well-constrained and well distributed observational tie points beneath the ice shelves, and around their margins.

4.3 Implications for the Amundsen Sea ice shelves

4.3.1 Pathways for water

The results of our new bathymetric estimates have significant implications for how we understand the pattern of cryospheric changes occurring in the Thwaites, Dotson and Crosson areas. Our primary observation confirms that the ice front in the centre of Thwaites Glacier is directly and easily accessible to mCDW through a channel over 800 m deep beneath the Thwaites Eastern Ice Shelf and Thwaites Glacier Tongue (Millan et al., 2017;Tinto and Bell, 2011) (Fig. 2a). This trough is separated from an adjacent >1000 m deep trough by a ridge that is in places <150 m deep where the Eastern Ice Shelf and Thwaites Glacier Tongue ~~grounded~~were pinned. However, 700 to 800 m deep channels cut the ridge, linking the two troughs, and potentially facilitating lateral circulation beneath the ice shelves. Warm mCDW is dense, and could be filling the bathymetric depressions and troughs on the continental shelf we observe, transporting heat from the global ocean to interact with ice shelves and contributing to ice sheet grounding line melting~~As mCDW is warmer than the typical shelf water, its circulation can contribute to ice shelf and ice sheet grounding line melting~~ (Jenkins et al., 2010).

The Crosson Ice Shelf is underlain by bathymetry 300 to 500 m deep, shallower than the typical core of the mCDW (Assmann et al., 2013). A 700 – 1000 m deep channel is present flanking Bear Island (Figs. 2b and 3c), but its width of just 10 km suggests that the flux of mCDW may be less via this route. However, in some years the upper boundary of the mCDW can sit around 400-600 m deep (Dutrieux et al., 2014;Jenkins et al., 2018), shallower than much of the bathymetry beneath the Crosson Ice Shelf, meaning mCDW could still access the inner Crosson cavity. The final ~30 km to the most recent grounding line of Smith Glacier are characterised by a cavity typically 100-200 m thick.~~,~~ As models indicate that reduced cavity thickness can supress strong oceanic circulation (Seroussi et al., 2017) this ~~which~~ could limit the supply of mCDW water to the grounding line. The Dotson Ice Shelf is underlain by a broad cavity >800 m deep and is separated from the currently rapidly-changing

grounding line of the western branch of the Kohler Glacier by a sill 700-800 m deep (Fig. 3d). This sill may partially shield this grounding line from oceanographically-driven change, as the bulk of the inflowing mCDW is mapped at a depth of ~800 m at the Dotson ice shelf margin (Miles et al., 2016).

4.3.2 Two ice shelf populations

A second key observation is that the ice shelves in areas which ungrounded since measurement of the 1993 grounding line are all underlain by relatively thin cavities (Fig. 2b). Such thin cavity geometry in newly un-grounded regions is predicted by some fully coupled, ice-ocean numerical models of ice sheet retreat (Seroussi et al., 2017). These newly formed regions of floating ice (Fig. 1d) appear to be distinct from the wider, more established, ice shelf system which is underlain by both thick and thin cavities. This pattern is not simply a result of distance, and hence time since crossing ~~from~~ the grounding line, as in places where the ice shelf has not ~~retreated~~ advanced inland thick cavities are seen at the grounding line, for example west of Thwaites Glacier tongue, and East of Pope Glacier (Fig. 2b). To consider the different ice shelf systems in more detail we plotted hydrostatic ice shelf draft against our recovered bathymetry (Fig. 5). The older ice shelves, outboard from the 1993 grounding line, show limited correlation with the underlying bathymetry (Fig. 5a). This is expected given the shelves float passively over the underlying topography. Regionally the main control on the draft of these ice shelves is likely the depth of top of the mCDW, which ~~would~~ drives enhanced basal melt. The fact that few of the older ice shelves have depths greater than 500 m ~~would be~~is consistent with this hypothesis, as mCDW at depths of 400 to 800 m is observed in oceanographic transects at the ice shelf edge (Miles et al., 2016;Dutrieux et al., 2014;Jenkins et al., 2018;Jacobs et al., 1996). ~~The slight positive correlation between depth and thinner ice shelves (Fig. 5a) may reflect shallower bathymetry forcing mCDW to shallower levels.~~

The draft in newly established ice shelf areas shows an almost 1:1 relationship with the underlying bathymetry (Fig. 5b). The difference between the bed elevation and ice shelf draft suggests that these newly formed cavities are on average 112 m thick, with >95% being <~400 m thick. The rapid grounding line retreat which led to the formation of the post-1993 ice shelf sectors has been regarded as a harbinger of catastrophic collapse of the Amundsen Sea sector of the West Antarctic Ice Sheet through geometric marine ice sheet instability, unconstrained by inland pinning points (Rignot et al., 2014). It has been suggested that basal melting driven by ingress of warmer mCDW could be a key factor facilitating this process (Milillo et al., 2019;Pritchard et al., 2012). ~~Our results indicate there is generally a close relationship between bed elevation, cavity thickness and ice shelf draft in the newly un-grounded regions. We consider two end-member conceptual mechanisms which could have driven the rapid grounding line retreat and development of the observed cavity geometry; ice flow acceleration coupled with geometric spreading, or enhanced grounding line melt (Fig. 6).~~

~~In the case of geometric spreading (Fig. 6a), accelerating ice flow means the ice sheet thins. As the ice sheet reaches its hydrostatic limit it un-grounds. When this occurs on a retrograde bed, as is the case for the majority of our study region (Fig. 3), the non-linear dependence of the ice flow speed across the grounding line on the ice thickness facilitates further acceleration and un-grounding (Schoof, 2007). The process of acceleration could be initiated by un-grounding of a buttressing ice shelf from critical pinning points, or ice shelf thinning due to enhanced basal melting. This mechanism can explain rapid grounding~~

~~line retreat, without the need for sustained penetration of warm ocean water through a narrow sub-ice shelf cavity. However, in this scenario there is no clear mechanism for maintaining a cavity with a relatively uniform thickness following the underlying topography once the system is un-grounded.~~

~~Where grounding line retreat is driven by melting, very high melt rates are likely focused at the grounding line (Fig. 6b) (Lilien et al., 2019). This could reflect the first interaction between warm saline mCDW, the front of the grounded ice sheet and fresh subglacial melt water if any exists (Fig. 6b). In our conceptual model enhanced basal melting remains focused at the grounding line until the ice thins enough to un-ground. The enhanced melting zone moves further inboard with the grounding line, and negative feedbacks such as cooling and dilution of the mCDW, and the higher pressure melting temperature at shallower depths inhibits further significant erosion of the cavity.~~ Enhanced basal melting of up to 200 m per year has been calculated from satellite observations and OIB radar profiles over the new Thwaites Glacier ice shelves (Milillo et al., 2019), and rates of 50-70 m a^{-1} have been observed close to the grounding line of Smith Glacier (Khazendar et al., 2016). However, our data indicate that the highest of these melt rates must be ~~spatially limited~~restricted to the grounding line, as the newly formed cavity thickness typically does not exceed ~400 m, i.e. approximately two years of the most elevated melt rates, and 8 years at the lower end of the enhanced melt rates. We propose that the fast flowing ice is advected across the region of most enhanced melting, limiting subsequent thinning ~~and preserving~~of the cavity. This is in line with the suggestion of previous authors that where grounding line retreat is driven by melting, very high melt rates are likely focused at the grounding line (Lilien et al., 2019).

In the Smith Glacier region comparison of 2016 OIB radar with earlier radar data allows reconstruction of the spatial distribution of the most recent ice shelf thinning (Fig. ~~7~~6). These direct observations confirm, as predicted from our cavity thickness estimate, that across much of the new ice shelf, thinning rates are relatively low, hence a relatively thin cavity can be maintained. However, they also reveal that the enhanced thinning rates of 50-70 m a^{-1} beneath the inner shelf noted for the period 2002 to 2009 (Khazendar et al., 2016) have continued into the period 2009-2016. These high rates appear to be restricted to the area where the base of the ice shelf is >1200 m deep. One possibility is that mCDW is penetrating to the grounding line and pooling at these depths. However,~~, but~~ it is not clear to what extent this water would have been mixed and diluted during its passage through the <400 m thick sub-ice shelf cavity. Also, ~~the~~ ice-shelf marginal weakening and consequent ice acceleration ~~likely~~ may have also contributed to the observed fast grounding-line retreat and thinning at the grounding line without the need for such extreme basal melting (Lilien et al., 2019).

~~We do not consider the geometric or basal melt mechanisms outlined above to be mutually exclusive. However, t~~The consistent presence of broad but vertically thin subglacial cavities appears to ~~be most challenging~~ challenge ~~for~~ a purely melt driven model of future ice sheet collapse, as access by warm water to the grounding line would be hampered by the thin cavity (Schoof, 2007). This physical limitation is supported by models for Pine Island Glacier margin, which indicated that cavities <200 m thick slowed the ingress of warm bottom water over topographic ridges (De Rydt et al., 2014). More complex fully coupled ocean-ice models also show the development of thin cavities and indicate that the associated weak circulation acts to slow grounding line retreat relative to that predicted by an un-coupled model (Seroussi et al., 2017).

The contrast in cavity geometry and relationship to the underlying bathymetry of the pre and post 1993 ice shelf regions suggests that the recently un-grounded regions may not yet be in equilibrium with the wider glaciological and oceanic system. As such, they may play a significant, but as yet poorly understood role in controlling the future evolution of the ice sheet marginal system. The thin cavities in particular may act to slow future changes. Firstly, they place a fundamental limit onto the amount of warm water which can flux beneath the glacier, and may also facilitate the tidally-driven turbulent flow mixing of water masses before they can reach the grounding line (Holland, 2008). In addition, the thin cavities which we observe are particularly sensitive to re-grounding on retrograde slopes, a negative feedback which would act to temporally re-stabilise a retreating ice sheet, a process which would be favoured by the observed rapid uplift due to glacial isostatic adjustment (Barletta et al., 2018). ~~This~~ The process of grounding line re-advance appears to have occurred in the Western Kohler Glacier (Fig. 1a), where the 2014 grounding line lies downstream of the 2012 grounding line (Rignot et al., 2014). Our observations of consistent thin cavities in newly un-grounded regions supports the results of coupled ocean-ice models confirming the necessity of such detailed modelling for predicting the evolution of the Thwaites Glacier system (Seroussi et al., 2017).

5. Conclusions

Airborne gravity provides a good first order estimate of sub-ice-shelf bathymetry. Despite the relatively high uncertainty (~100 m standard deviation) comparisons with different gravity inversion techniques, the location of ice shelf pinning points and new observational bathymetric data, indicate that the pattern of sub-ice-shelf bathymetry is well resolved.

Thwaites Glacier is connected to ~~the deep ocean~~Pine Island Bay to its east by a major trough >800 m deep and 20 km wide. In contrast the grounding lines of the of Dotson and Crosson ice shelves are accessible through relatively narrow channels and thin sub shelf cavities.

In the Thwaites, Dotson and Crosson region, areas of ice shelf which developed before and after 1993 form distinct populations. The most recently un-grounded areas are underlain by thin cavities (average 112 m) where the ice shelf base closely tracks the underlying bed topography. We propose that these systems represent a transient phase of ice margin development, which may act to slow future changes, which is indicated but not fully captured in present models.

Data availability

The new calculated bathymetry along with input topography and gravity grids is available from the UK Polar Data Centre (Jordan et al., 2020a). The associated ITGC line airborne ~~geophysical data~~ gravity and magnetic data is available from the same source ~~the UK Polar Data Centre upon publication of this paper~~ (Jordan et al., 2020b;Jordan et al., 2020c). ~~Input topography, gravity grids and model bathymetry will also be available from the same source(Jordan et al., 2020a).~~ Other data is from sources cited in the text.

Author Contributions

All authors contributed to the discussion and production of the final manuscript.

Additional specific contributions include:

Tom Jordan – Gravity data processing, topographic shift bathymetric inversion and primary manuscript preparation.

David Porter – Airborne gravity and magnetic data collection.

Kirsty Tinto – Discussion of bathymetry inversion techniques.

Romain Millan – Discussion of gravity inversion and preparation of gravity shift bathymetric model.

Atsuhiro Muto - Discussion of gravity inversion and implications of ice sheet cavity findings.

Kelly Hogan – Preparation of multibeam swath bathymetry.

Rob Larter – Provision of ship-borne gravity and mutlibeam swath data.

Ali Graham – processing and preparation of mutlibeam swath bathymetry data on NBP19-02.

John Paden – led airborne radar system development, data processing, and ice bottom tracking.

Competing Interests

None

Acknowledgements

This work is a British Antarctic Survey (BAS) National Capability contribution to the International Thwaites Glacier Collaboration (ITGC), with additional support from the BAS Geology and Geophysics Team (TJ). Additional support for this work is from Lamont-Doherty Earth Observatory NSF grant number NSF1842064 (DP, KT), and the THOR (KH, RL, AG, and Cruise NBP19 02), ~~and~~ TARSAN (AM) and MELT (JP) projects, components of the International Thwaites Glacier Collaboration (ITGC). Support from National Science Foundation (NSF: Grant NSFPLR-NERC-1738942 for THOR, NSFPLR-NERC-1738992 for TARSAN, NSFPLR-NERC-1739003 for MELT) and Natural Environment Research Council (NERC: Grant NE/S006664/1 for THOR, NE/S006419/1 for TARSAN). This is paper number ITGC:009.

References

Abulaitijiang, A., Andersen, O. B., and Sandwell, D.: Improved Arctic Ocean Bathymetry Derived From DTU17 Gravity Model, Earth and Space Science, 6, 1336-1347, 10.1029/2018EA000502, 2019.

An, L., Rignot, E., Millan, R., Tinto, K., and Willis, J.: Bathymetry of Northwest Greenland Using "Ocean Melting Greenland" (OMG) High-Resolution Airborne Gravity and Other Data, Remote Sensing, 11, https://doi.org/10.3390/rs11020131 2019.

Assmann, K. M., Jenkins, A., Shoosmith, D. R., Walker, D. P., Jacobs, S. S., and Nicholls, K. W.: Variability of Circumpolar Deep Water transport onto the Amundsen Sea Continental shelf through a shelf break trough, Journal of Geophysical Research: Oceans, 118, 6603-6620, 10.1002/2013JC008871, 2013.

Barletta, V. R., Bevis, M., Smith, B. E., Wilson, T., Brown, A., Bordoni, A., Willis, M., Khan, S. A., Rovira-Navarro, M., Dalziel, I., Smalley, R., Kendrick, E., Konfal, S., Caccamise, D. J., Aster, R. C., Nyblade, A., and Wiens, D. A.: Observed rapid bedrock uplift in Amundsen Sea Embayment promotes ice-sheet stability, Science, 360, 1335, 10.1126/science.aao1447, 2018.

Becker, D., Nielsen, J. E., Ayres-Sampaio, D., Forsberg, R., Becker, M., and Bastos, L.: Drift reduction in strapdown airborne gravimetry using a simple thermal correction, Journal of Geodesy, 89, 1133-1144, 2015.

Blankenship, D. D., Young, D., Holt, J. W., and D., K. S.: AGASEA Ice Thickness Profile Data from the Amundsen Sea Embayment, Antarctica. U.S. Antarctic Program (USAP) Data Center, 2012.

Brisbourne, A. M., Smith, A. M., King, E. C., Nicholls, K. W., Holland, P. R., and Makinson, K.: Seabed topography beneath Larsen C Ice Shelf from seismic soundings, The Cryosphere, 8, 1-13, 10.5194/tc-8-1-2014, 2014.

Cochran, J. R., and Bell, R. E.: IceBridge Sander AIRGrav L1B Geolocated Free Air Gravity Anomalies., Boulder, Colorado USA: NASA DAAC at the National Snow and Ice Data Center., 2010, updated 2018.

Cochran, J. R., and Bell, R. E.: Inversion of IceBridge gravity data for continental shelf bathymetry beneath the Larsen Ice Shelf, Antarctica, Journal of Glaciology, 58, 540-552, doi: 510.3189/2012JoG3111J3033, 2012.

Cochran, J. R., Jacobs, S. S., Tinto, K. J., and Bell, R. E.: Bathymetric and oceanic controls on Abbot Ice Shelf thickness and stability, The Cryosphere, 8, 877-889, 10.5194/tc-8-877-2014, 2014.

Davies, D., Bingham, R. G., Graham, A. G. C., Spagnolo, M., Dutrieux, P., Vaughan, D. G., Jenkins, A., and Nitsche, F. O.: High-resolution sub-ice-shelf seafloor records of twentieth century ungrounding and retreat of Pine Island Glacier, West Antarctica Journal of Geophysical Research, 122, 1698-1714. https://doi.org/1610.1002/2017JF004311, 2017.

De Rydt, J., Holland, P. R., Dutrieux, P., and Jenkins, A.: Geometric and oceanographic controls on melting beneath Pine Island Glacier, Journal of Geophysical Research: Oceans, 119, 2420-2438, 10.1002/2013JC009513, 2014.

Dutrieux, P., De Rydt, J., Jenkins, A., Holland, P. R., Ha, H. K., Lee, S. H., Steig, E. J., Ding, Q., Abrahamsen, E. P., and Schröder, M.: Strong Sensitivity of Pine Island Ice-Shelf Melting to Climatic Variability, Science, 343, 174, 10.1126/science.1244341, 2014.

Forste, C., Schmidt, R., Stubenvoll, R., Flechtner, F., Meyer, U., Konig, R., Neumayer, H., Biancale, R., Lemoine, J. M., Bruinsma, S., Loyer, S., Barthelmes, F., and Esselborn, S.: The Geo-ForschungsZentrum Potsdam/Groupe de Recherche de Geodesie Spatiale satellite-only and combined gravity field models:EIGEN-GL04S1 and EIGEN-GL04C, J. Geodesy, 82, 331–346,doi:310.1007/s00190-00007-00183-00198, 02008, 2008.

Fretwell, P., Pritchard, H. D., Vaughan, D. G., Bamber, J., Barrand, N., Bell, R., Bianchi, C., Bingham, R., Blankenship, D., Casassa, G., Callens, D., Conway, H., Cook, A. J., Corr, H. F. J., Damaske, D., Damm, V., Ferraccioli, F., Forsberg, R., Fujita, S., Gogineni, P., Griggs, J. A., Hindmarsh, R., Holmlund, P., Holt, J. W., Jacobel, R. W., Jenkins, A., Jokat, W., Jordan, T. A., King, E. C., Kohler, J., Krabill, W., Riger-Kusk, R., Langley, K. A., Leitchenkov, G., Leuschen, C., Luyendyk, B. P., Matsuoka, K., Nogi, Y., Nost, O. A., Popov, S., Rignot, E., Rippin, D. M., Riviera, A., Roberts, J., Ross, N., Siegert, M. J., Smith, A. M., Steinhage, D., Studinger, M., Sun, B., Tinto, B. K., Welch, B. C., Young, D. A., Xiangbin, C., and Zirizzotti, A.: Bedmap2: improved ice bed, surface and thickness datasets for Antarctica, The Cryosphere, 7, 2013.

Gardner, A. S., Moholdt, G., Scambos, T., Fahnstock, M., Ligtenberg, S., van den Broeke, M., and Nilsson, J.: Increased West Antarctic and unchanged East Antarctic ice discharge over the last 7 years, The Cryosphere, 12, 521-547, 10.5194/tc-12-521-2018, 2018.

Golynsky, A. V., Ferraccioli, F., Hong, J. K., Golynsky, D. A., Frese, R. R. B., Young, D. A., Blankenship, D. D., Holt, J. W., Ivanov, S. V., Kiselev, A. V., Masolov, V. N., Eagles, G., Gohl, K., Jokat, W., Damaske, D., Finn, C., Aitken, A., Bell, R. E., Armadillo, E., Jordan, T. A., Greenbaum, J. S., Bozzo, E., Caneva, G., Forsberg, R., Ghidella, M., Galindo-Zaldivar, J., Bohoyo, F., Martos, Y. M., Nogi, Y., Quartini, E., Kim, H. R., and Roberts, J. L.: New Magnetic Anomaly Map of the Antarctic, Geophysical Research Letters, 45, 6437-6449, doi:10.1029/2018GL078153, 2018.

Gómez-Ortiz, D., and Agarwal, B. N. P.: 3DINVER.M: a MATLAB program to invert the gravity anomaly over a 3D horizontal density interface by Parker–Oldenburg's algorithm, Computers & Geosciences, 31, 513-520, https://doi.org/10.1016/j.cageo.2004.11.004, 2005.

Graham, A. G. C., Larter, R. D., Gohl, K., Hillenbrand, C.-D., Smith, J. A., and Kuhn, G.: Bedform signature of a West Antarctic palaeo-ice stream reveals a multi-temporal record of flow and substrate control, Quaternary Science Reviews, 28, 2774-2793, https://doi.org/10.1016/j.quascirev.2009.07.003, 2009.

Griggs, J. A., and Bamber, J. L.: Antarctic ice-shelf thickness from satellite radar altimetry, Journal of Glaciology, 57, 485-498, 10.3189/002214311796905659, 2011.

Hodgson, D. A., Jordan, T. A., De Rydt, J., Fretwell, P. T., Seddon, S. A., Becker, D., Hogan, K. A., Smith, A. M., and Vaughan, D. G.: Past and future dynamics of the Brunt Ice Shelf from seabed bathymetry and ice shelf geometry, The Cryosphere, 13, 545-556, 10.5194/tc-13-545-2019, 2019.

Hogan, K. A., Larter, R. D., Graham, A. G. C., Arthern, R., Kirkham, J. D., Totten Minzoni, R., Jordan, T. A., Clark, R., Fitzgerald, V., Anderson, J. B., Hillenbrand, C. D., Nitsche, F. O., Simkins, L., Smith, J. A., Gohl, K., Arndt, J. E., Hong, J., and Wellner, J.: Revealing the former bed of Thwaites Glacier using sea-floor bathymetry, The Cryosphere Discuss., 2020, 1-36, 10.5194/tc-2020-25, 2020.

Holland, P. R.: A model of tidally dominated ocean processes near ice shelf grounding lines, Journal of Geophysical Research: Oceans, 113, 10.1029/2007JC004576, 2008.

Holt, J. W., Blankenship, D. D., Morse, D. L., Young, D. A., Peters, M. E., Kempf, S. D., Richter, T. G., Vaughan, A. P. M., and Corr, H.: New Boundary Conditions for the West Antarctic Ice Sheet: Subglacial Topography of the Thwaites and Smith Glacier Catchments., Geophysical Research Letters, 33, doi:10.1029/2005GL025561, 2006.

Howat, I. M., Porter, C., Smith, B. E., Noh, M. J., and Morin, P.: The Reference Elevation Model of Antarctica, The Cryosphere, 13, 665-674, 10.5194/tc-13-665-2019, 2019.

Jacobs, S. S., Hellmer, H. H., and Jenkins, A.: Antarctic Ice Sheet melting in the southeast Pacific, Geophysical Research Letters, 23, 957-960, 10.1029/96GL00723, 1996.

Jacobs, S. S., Jenkins, A., Giulivi, C. F., and Dutrieux, P.: Stronger ocean circulation and increased melting under Pine Island Glacier ice shelf., Nature Geosci, 4, 519–523, 2011.

Jenkins, A., Dutrieux, P., Jacobs, S. S., McPhail, S. D., Perrett, J. R., Webb, A. T., and White, D.: Observations beneath Pine Island Glacier in West Antarctica and implications for its retreat, Nature Geoscience, 3, 468 - 472. doi:410.1038/ngeo1890, 2010.

Jenkins, A., Shoosmith, D., Dutrieux, P., Jacobs, S., Kim, T. W., Lee, S. H., Ha, H. K., and Stammerjohn, S.: West Antarctic Ice Sheet retreat in the Amundsen Sea driven by decadal oceanic variability, Nature Geoscience, 11, 733-738, 10.1038/s41561-018-0207-4, 2018.

Jordan, T., Porter, D., Tinto, K., Millan, R., Muto, A., Hogan, K., Larter, R., Graham, A., Paden, J., and Robinson, C.: Gravity-derived bathymetry for the Thwaites, Crosson and Dotson ice shelves (2009-2019) (Version 1.0) Natural Environment Research Council, UK Research & Innovation, UK Polar Data Centre, 2020a.

Jordan, T., Robinson, C., and Porter, D.: Processed line aeromagnetic data over the Thwaites glacier region (2018/19 season). Natural Environment Research Council, UK Research & Innovation, UK Polar Data Centre, 2020b.

Jordan, T. A., and Becker, D.: Investigating the distribution of magmatism at the onset of Gondwana breakup with novel strapdown gravity and aeromagnetic data, Physics of the Earth and Planetary Interiors, 282, 77-88, https://doi.org/10.1016/j.pepi.2018.1007.1007, 2018.

Jordan, T. A., Robinson, C., Porter, D., Locke, C., and Tinto, K.: Processed line aerogravity data over the Thwaites Glacier region (2018/19 season). Natural Environment Research Council, UK Research & Innovation, UK Polar Data Centre, 2020c.

Joughin, I., Smith, B. E., and Medley, B.: Marine Ice Sheet Collapse Potentially Under Way for the Thwaites Glacier Basin, West Antarctica, Science, 344, 735-738, 10.1126/science.1249055, 2014.

Khazendar, A., Rignot, E., Schroeder, D. M., Seroussi, H., Schodlok, M. P., Scheuchl, B., Mouginot, J., Sutterley, T. C., and Velicogna, I.: Rapid submarine ice melting in the grounding zones of ice shelves in West Antarctica, Nature Communications, 7, 13243, 10.1038/ncomms13243, 2016.

Larter, R. D., Graham, A. G. C., Gohl, K., Kuhn, G., Hillenbrand, C.-D., Smith, J. A., Deen, T. J., Livermore, R. A., and Schenke, H.-W.: Subglacial bedforms reveal complex basal regime in a zone of paleo–ice stream convergence, Amundsen Sea embayment, West Antarctica, Geology, 37, 411-414, 10.1130/G25505A.1, 2009.

Lilien, D. A., Joughin, I., Smith, B., and Gourmelen, N.: Melt at grounding line controls observed and future retreat of Smith, Pope, and Kohler glaciers, The Cryosphere, 13, 2817-2834, 10.5194/tc-13-2817-2019, 2019.

Miles, T., Lee, S. H., Wåhlin, A., Ha, H. K., Kim, T. W., Assmann, K. M., and Schofield, O.: Glider observations of the Dotson Ice Shelf outflow, Deep Sea Research Part II: Topical Studies in Oceanography, 123, 16-29, https://doi.org/10.1016/j.dsr2.2015.08.008, 2016.

Milillo, P., Rignot, E., Rizzoli, P., Scheuchl, B., Mouginot, J., Bueso-Bello, J., and Prats-Iraola, P.: Heterogeneous retreat and ice melt of Thwaites Glacier, West Antarctica, Science Advances, 5, eaau3433, 10.1126/sciadv.aau3433, 2019.

Millan, R., Rignot, E., Bernier, V., Morlighem, M., and Dutrieux, P.: Bathymetry of the Amundsen Sea Embayment sector of West Antarctica from Operation IceBridge gravity and other data, Geophysical Research Letters, 44, 1360-1368, 10.1002/2016GL072071, 2017.

Morlighem, M., Rignot, E., Binder, T., Blankenship, D., Drews, R., Eagles, G., Eisen, O., Ferraccioli, F., Forsberg, R., Fretwell, P., Goel, V., Greenbaum, J. S., Gudmundsson, H., Guo, J., Helm, V., Hofstede, C., Howat, I., Humbert, A., Jokat, W., Karlsson, N. B., Lee, W. S., Matsuoka, K., Millan, R., Mouginot, J., Paden, J., Pattyn, F., Roberts, J., Rosier, S., Ruppel, A., Seroussi, H., Smith, E. C., Steinhage, D., Sun, B., Broeke, M. R. v. d., Ommen, T. D. v., Wessem, M. v., and Young, D. A.: Deep glacial troughs and stabilizing ridges unveiled beneath the margins of the Antarctic ice sheet, Nature Geoscience, 13, 132-137, 10.1038/s41561-019-0510-8, 2020.

Muto, A., Peters, L. E., Gohl, K., Sasgen, I., Alley, R. B., Anandakrishnan, S., and Riverman, K. L.: Subglacial bathymetry and sediment distribution beneath Pine Island Glacier ice shelf modeled using aerogravity and in situ geophysical data: New results, Earth and Planetary Science Letters, 433, 63-75, http://dx.doi.org/10.1016/j.epsl.2015.10.037, 2016.

Nitsche, F. O., Gohl, K., Larter, R. D., Hillenbrand, C. D., Kuhn, G., Smith, J. A., Jacobs, S., Anderson, J. B., and Jakobsson, M.: Paleo ice flow and subglacial meltwater dynamics in Pine Island Bay, West Antarctica, The Cryosphere, 7, 249-262, 10.5194/tc-7-249-2013, 2013.

Paden, J., Li, J., Leuschen, C., Rodriguez-Morales, F., and Hale, R.: IceBridge MCoRDS L2 Ice Thickness, Version 1., NASA (Ed.), NASA National Snow and Ice Data Center Distributed Active Archive Center., Boulder, Colorado USA, 2010, updated 2018.

Pail, R., Goiginger, H., Mayrhofer, R., Schuh, W. D., Brockmann, J. M., Krasbutter, I., Höck, E., and Fecher, T.: GOCE gravity field model derived from orbit and gradiometery data applying the time-wise method, ESA Living Planet Symposium, Bergen, Norway, 2010,

Pritchard, H. D., Ligtenberg, S. R. M., Fricker, H. A., Vaughan, D. G., van den Broeke, M. R., and Padman, L.: Antarctic ice-sheet loss driven by basal melting of ice shelves, Nature, 484, 502-505, 10.1038/nature10968, 2012.

Rignot, E., Mouginot, J., and Scheuchl, B.: Antarctic grounding line mapping from differential satellite radar interferometry, Geophysical Research Letters, 38, 10.1029/2011GL047109, 2011.

Rignot, E., Mouginot, J., Morlighem, M., Seroussi, H., and Scheuchl, B.: Widespread, rapid grounding line retreat of Pine Island, Thwaites, Smith, and Kohler glaciers,West Antarctica, from 1992 to 2011, Geophysical Research Letters, 41, 3502-3409, DOI: 3510.1002/2014GL060140, 2014.

Rignot, E., Mouginot, J., and Scheuchl, B.: MEaSUREs InSAR-Based Antarctica Ice Velocity Map, Version 2. . NASA National Snow and Ice Data Center Distributed Active Archive Center. , Boulder, Colorado USA., 2017.

Rosier, S. H. R., Hofstede, C., Brisbourne, A. M., Hattermann, T., Nicholls, K. W., Davis, P. E. D., Anker, P. G. D., Hillenbrand, C.-D., Smith, A. M., and Corr, H. F. J.: A New Bathymetry for the Southeastern Filchner-Ronne Ice Shelf: Implications for Modern Oceanographic Processes and Glacial History, Journal of Geophysical Research: Oceans, 123, 4610-4623, doi:10.1029/2018JC013982, 2018.

Roy, L., Sen, M. K., Blankenship, D. D., Stoffa, P. L., and Richter, T. G.: Inversion and uncertainty estimation of gravity data using simulated annealing: An application over Lake Vostok, East Antarctica, Geophysics, 70, J1-J12, 10.1190/1.1852777, 2005.

Scambos, T. A., Bohlander, J. A., Shuman, C. A., and Skvarca, P.: Glacier acceleration and thinning after ice shelf collapse in the Larsen B embayment, Antarctica, Geophysical Research Letters, 31, doi:10.1029/2004GL020670, 2004.

Scambos, T. A., Bell, R. E., Alley, R. B., Anandakrishnan, S., Bromwich, D. H., Brunt, K., Christianson, K., Creyts, T., Das, S. B., DeConto, R., Dutrieux, P., Fricker, H. A., Holland, D., MacGregor, J., Medley, B., Nicolas, J. P., Pollard, D., Siegfried, M. R., Smith, A. M., Steig, E. J., Trusel, L. D., Vaughan, D. G., and Yager, P. L.: How much, how fast?: A science review and outlook for research on the instability of Antarctica's Thwaites Glacier in the 21st century, Global and Planetary Change, 153, 16-34, https://doi.org/10.1016/j.gloplacha.2017.04.008, 2017.

Schoof, C.: Ice sheet grounding line dynamics: steady states, stability and hysteresis, Journal of Geophysical Research, 112, F03S28, doi:10.1029/2006JF000664, 2007.

Seroussi, H., Nakayama, Y., Larour, E., Menemenlis, D., Morlighem, M., Rignot, E., and Khazendar, A.: Continued retreat of Thwaites Glacier, West Antarctica, controlled by bed topography and ocean circulation, Geophysical Research Letters, 44, 6191-6199, 10.1002/2017GL072910, 2017.

Smith, W. H. F., and Wessel, P.: Gridding with continuous curvature splines in tension, Geophysics, 55, 293-305, 1990.

Smith, W. H. F., and Sandwell, D. T.: Bathymetric prediction from dense satellite altimetry and sparse shipboard bathymetry, Journal of Geophysical Research: Solid Earth, 99, 21803-21824, 10.1029/94JB00988, 1994.

Studinger, M., Bell, R., and Frearson, N.: Comparison of AIRGrav and GT-1A airborne gravimeters for research applications, Geophysics, 73, 151-161, 2008.

Telford, W. M., Geldart, L. P., and Sheriff, R. E.: Applied Geophysics, 2nd ed., Cambridge University Press, Cambridge, 1990.

Tinto, K., Bell, R. E., and Cochran, J. R.: IceBridge Sander AIRGrav L3 Bathymetry, Version 1., NASA National Snow and Ice Data Center Distributed Active Archive Center., Boulder, Colorado USA., 2011.

Tinto, K. J., and Bell, R. E.: Progressive unpinning of Thwaites Glacier from newly identified offshore ridge: Constraints from aerogravity, Geophysical Research Letters, 38, DOI: 10.1029/2011GL049026, 2011.

Tinto, K. J., Padman, L., Siddoway, C. S., Springer, S. R., Fricker, H. A., Das, I., Caratori Tontini, F., Porter, D. F., Frearson, N. P., Howard, S. L., Siegfried, M. R., Mosbeux, C., Becker, M. K., Bertinato, C., Boghosian, A., Brady, N., Burton, B. L., Chu, W., Cordero, S. I., Dhakal, T., Dong, L., Gustafson, C. D., Keeshin, S., Locke, C., Lockett, A., O'Brien, G., Spergel, J. J., Starke, S. E., Tankersley, M., Wearing, M. G., and Bell, R. E.: Ross Ice Shelf response to climate driven by the tectonic imprint on seafloor bathymetry, Nature Geoscience, 12, 441-449, 10.1038/s41561-019-0370-2, 2019.

von Frese, R. R. B., Hinze, W. J., Braile, L. W., and Luca, A. J.: Spherical earth gravity and magnetic anomaly modeling by Gauss- Legendre quadrature integration, Journal of Geophysics, 49, 234-242, 1981.

Weertman, J.: Stability of the junction of an ice sheet and an ice shelf, Journal of Glaciology, 13, 3-11, 1974.

Wei, M., and Schwarz, K. P.: Flight test results from a strapdown airborne gravity system, Journal of Geodesy, 72, 323-332, 1998.

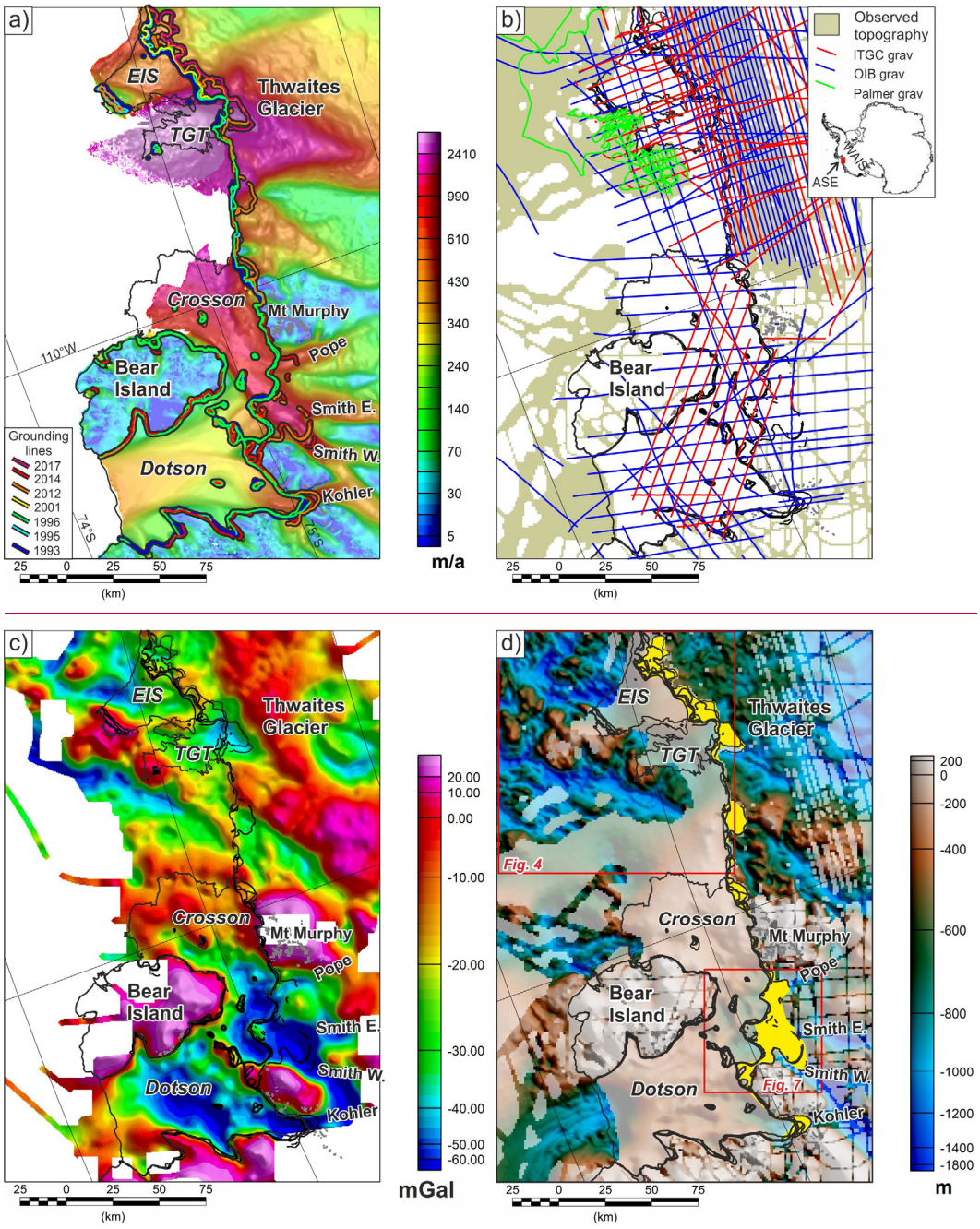
a)
EIS
Thwaites Glacier
TGT
Crosson
Mt Murphy
Pope
Bear Island
Smith E.
Smith W.
Dotson
Kohler
110°W
74°S
75°S
Grounding lines
2017
2014
2012
2001
1996
1995
1993
25 0 25 50 75
(km)
2410
990
610
430
340
240
140
70
30
5
m/a
b)
Observed topography
ITGC grav
OIB grav
Palmer grav
WAIS
ASE
Bear Island
25 0 25 50 75
(km)
c)
EIS
Thwaites Glacier
TGT
Crosson
Mt Murphy
Pope
Bear Island
Smith E.
Smith W.
Dotson
Kohler
25 0 25 50 75
(km)
20.00
10.00
0.00
-10.00
-20.00
-30.00
-40.00
-50.00
-60.00
mGal
d)
EIS
Thwaites Glacier
TGT
Fig. 4
Crosson
Mt Murphy
Pope
Bear Island
Smith E.
Smith W.
Fig. 7
Dotson
Kohler
25 0 25 50 75
(km)
200
0
-200
-400
-600
-800
-1000
-1200
-1400
-1800
m

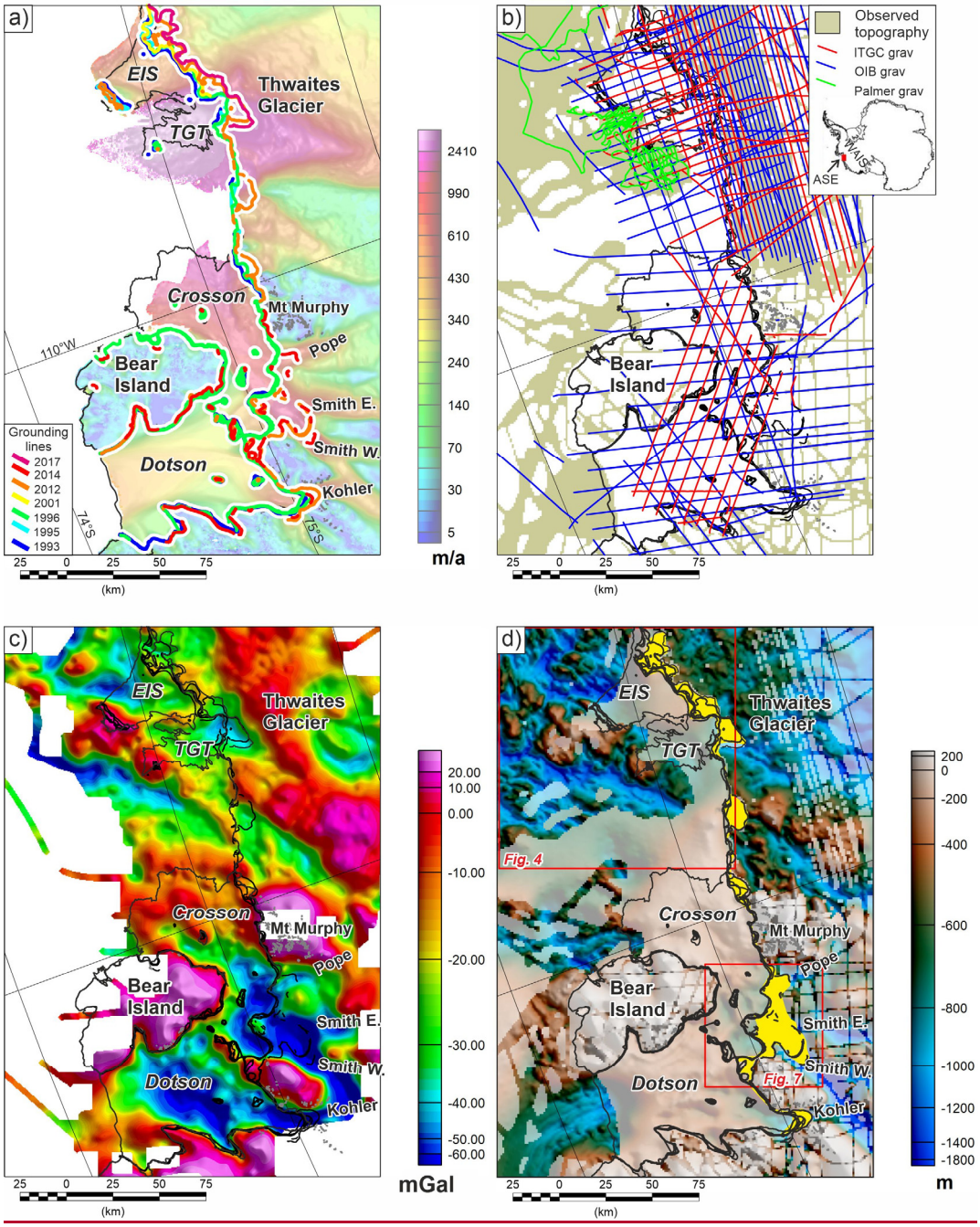

Figure 1: Regional setting and input data. a) Ice velocity (Rignot et al., 2017) with InSAR grounding lines in colour (Rignot et al., 2014;Milillo et al., 2019). Grey lines rock exposures. Thwaites Glacier Tongue (TGT), Eastern ice Shelf (EIS). b) Line gravity data coverage, regions of known topography and inset showing Antarctic context. ASE is Amundsen Sea Embayment, WAIS West Antarctic Ice Sheet. c) Integrated free air gravity anomaly grid. d) Direct topographic observations (strong colours), onshore from Operation Ice Bridge (OIB) (Paden et al., 2010, updated 2018) and ITGC, and offshore from ship-borne swath coverage (Hogan et al. 2020). Pale colours show BEDMAP2 DEM (Fretwell et al., 2013). Yellow areas highlight post 1993 ice shelves. Red boxes locate figures 4 and 7.

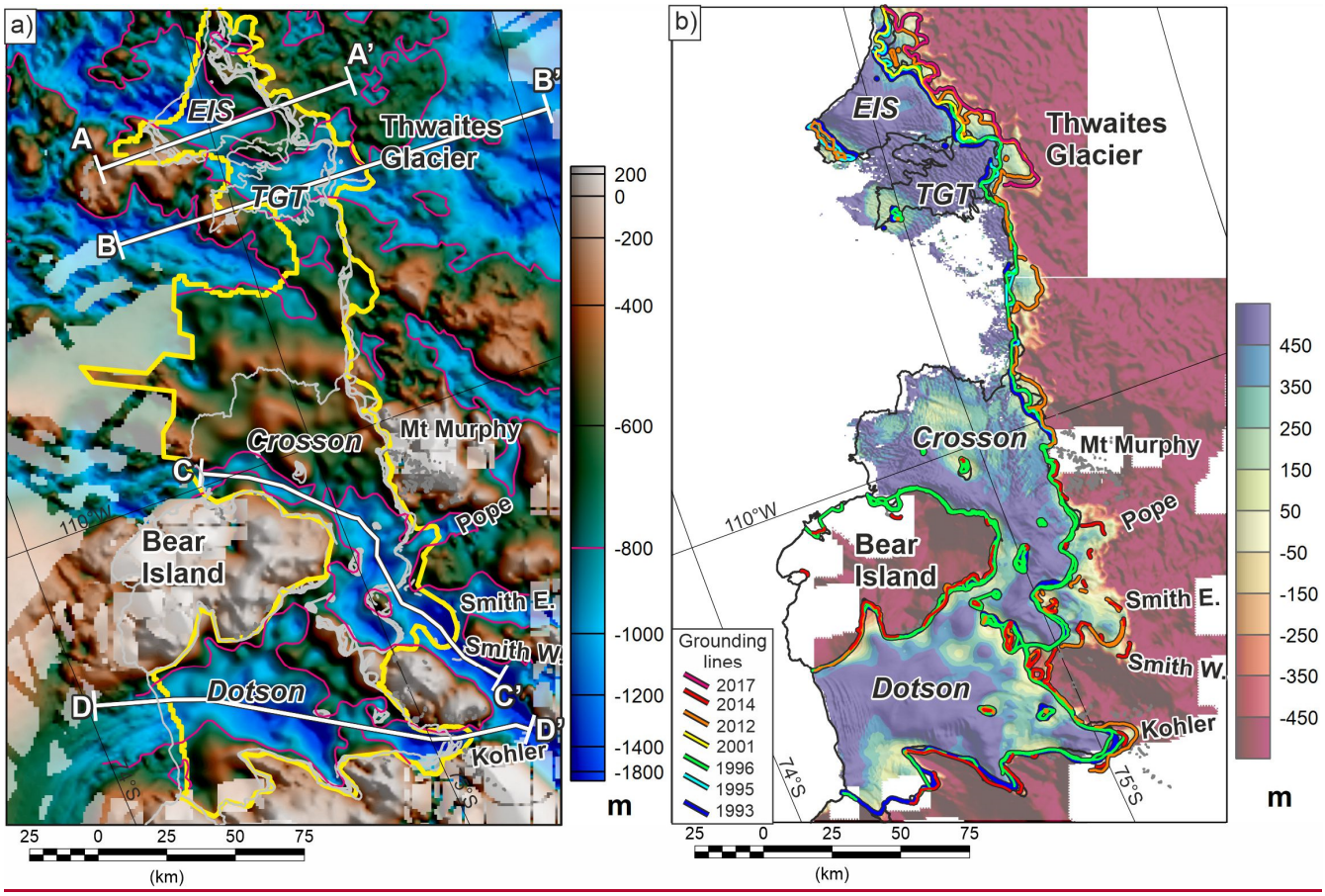
a)
A
A'
B
B'
EIS
Thwaites Glacier
TGT
Crosson
Mt Murphy
C
C'
Pope
Bear Island
Smith E.
Smith W.
D
D'
Dotson
Kohler
110°W
200
0
-200
-400
-600
-800
-1000
-1200
-1400
-1800
m
25 0 25 50 75
(km)
b)
EIS
Thwaites Glacier
TGT
Crosson
Mt Murphy
Pope
Bear Island
Smith E.
Smith W.
Dotson
Kohler
110°W
74°S
75°S
Grounding lines
2017
2014
2012
2001
1996
1995
1993
450
350
250
150
50
-50
-150
-250
-350
-450
m
25 0 25 50 75
(km)

590

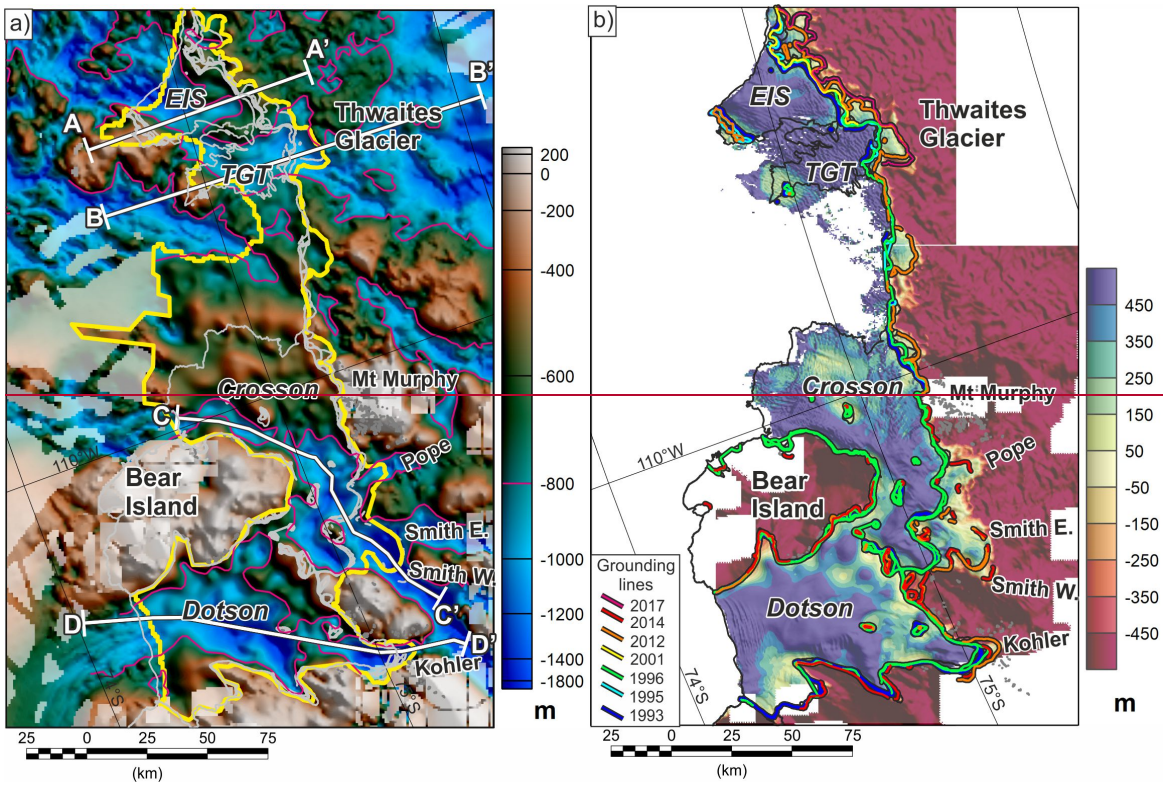

Figure 2: New bathymetry and cavity maps. a) Final topography from terrain shift method. White lines A-D mark profiles in Fig. 3. Yellow outline encloses region constrained by gravity data. Pink line shows -800m depth contour. Light grey lines mark grounding lines and ice shelf edge. b) Sub-ice-shelf water column thickness based on the REMA DEM and an assumption of hydrostatic equilibrium. Regions where the ice sheet is predicted to be grounded show negative cavity thickness.

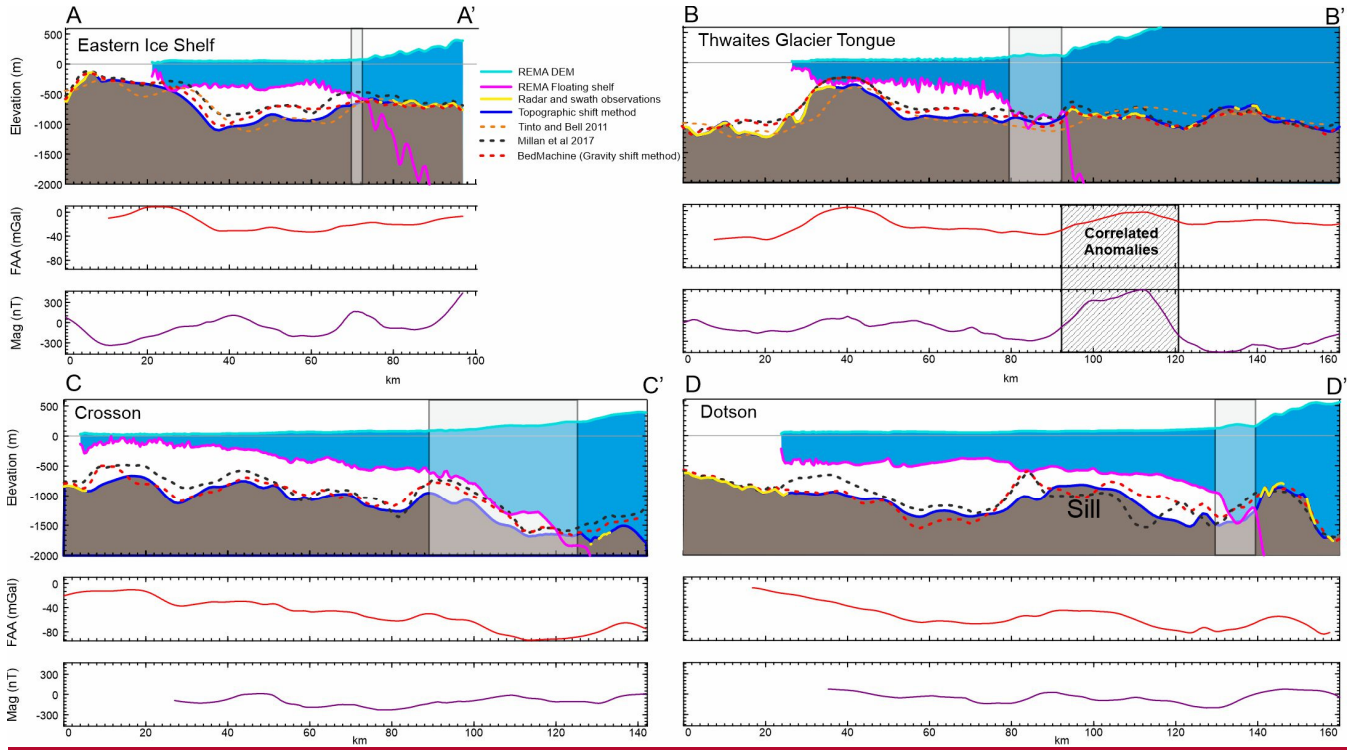

Figure 3: Profiles across ice shelves. Upper panel shows ice surface from REMA DEM (Howat et al., 2019) and base of ice shelf calculated assuming hydrostatic equilibrium, together with gravity-derived bathymetric estimates. Second panel shows input free-air gravity anomaly. Third panel shows magnetic anomalies derived from ITGC survey data ~~(REF data doi)~~(Jordan et al., 2020b) and ADMAP2 (Golynsky et al., 2018). a) Thwaites Eastern Ice Shelf. b) Thwites Glacier Tongue. c) Crosson Ice Shelf. d) Dotson Ice Shelf. Note thin cavity in regions of ice sheet grounding line retreat since 1993 (grey boxes in upper panels). Also in (d) note >500 m bathymetric highs in BedMachine and Millan (2017) profiles not associated with a free air gravity anomaly, indicative of artefacts resulting from the inversion process.

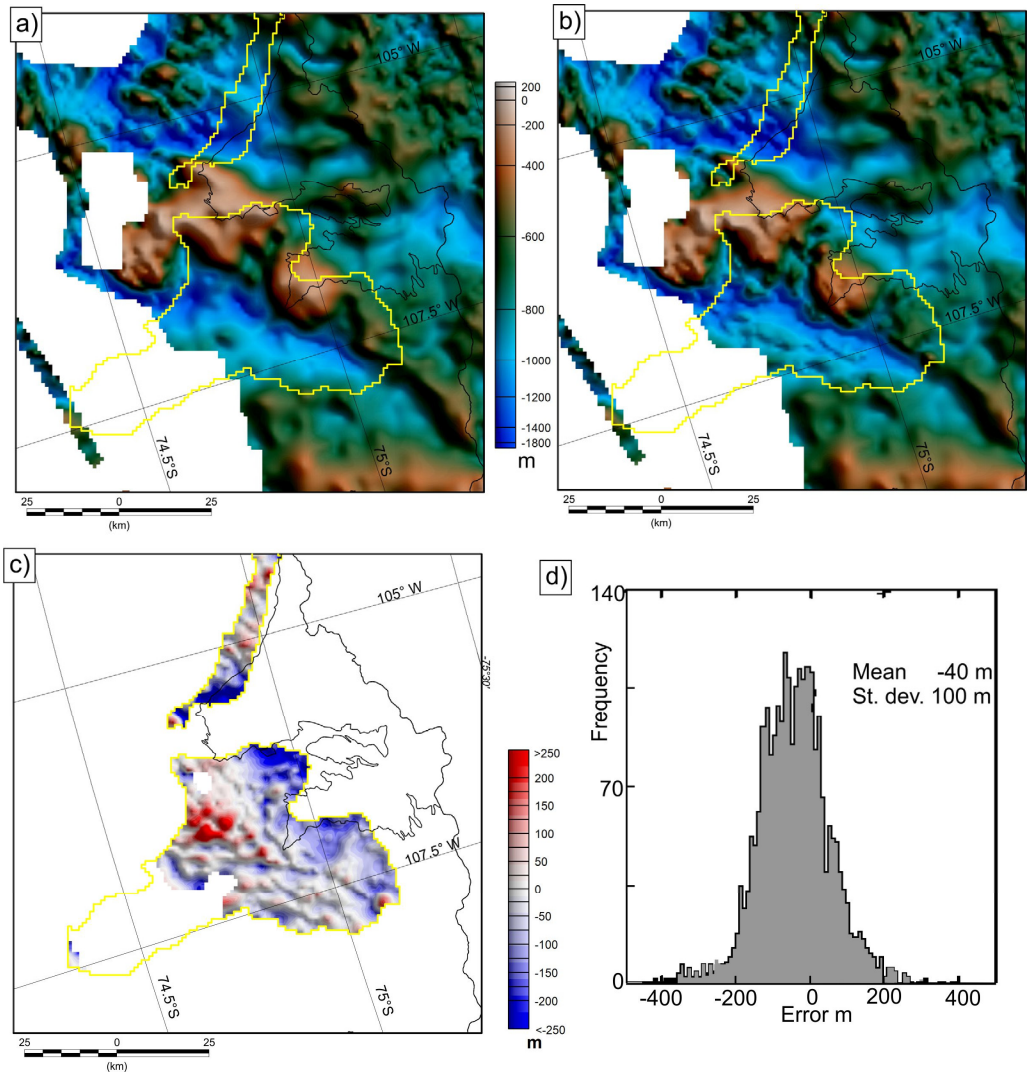

Figure 4: Error estimates. a) Bathymetric estimate excluding bathymetric data from cruises NBP19-02 and JR294 (yellow outlines). b) Bathymetry including new multibeam data (as in Fig. 2a). c) Discrepancy in areas of additional data. d) Histogram of errors in areas of new multibeam constraint.

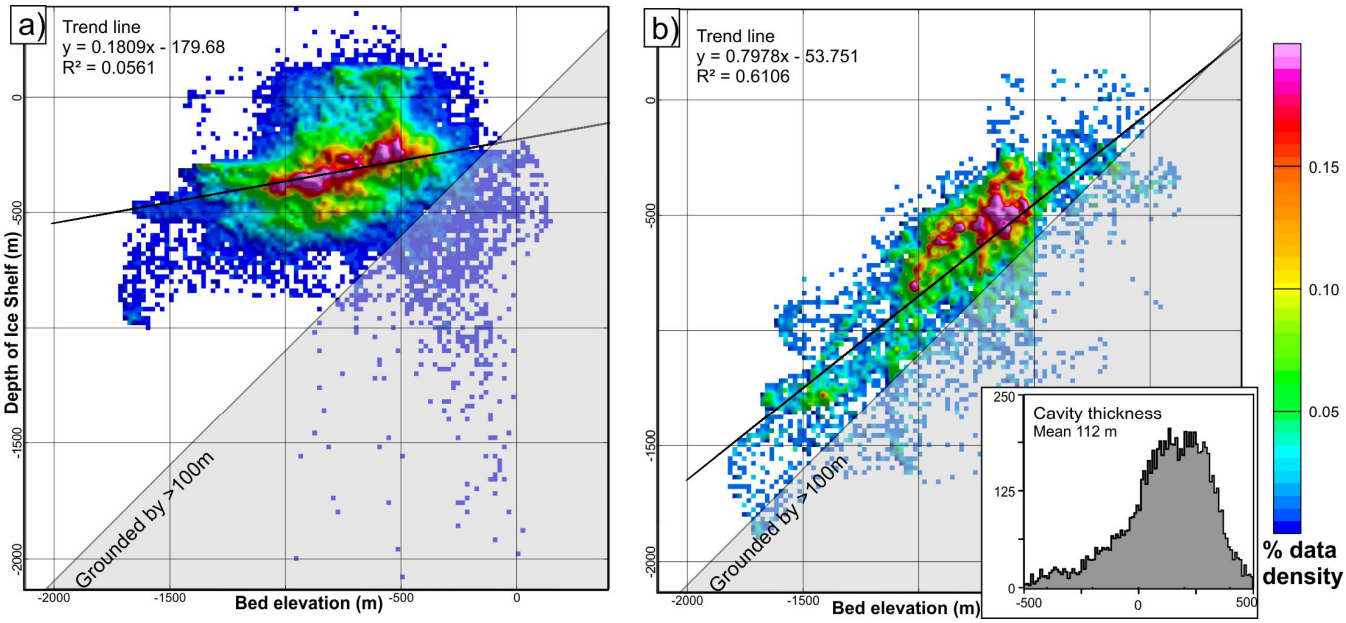

Figure 5: Data density plot of hydrostatic ice shelf draft against sub-shelf bathymetry. Trend lines show best linear fit through data point cloud. a) Plot for ice shelves outboard of the 1993 grounding line. b) Plot for ice shelves formed by grounding line retreat since 1993, with inset showing histogram of cavity thickness beneath the areas of newly developed ice shelf. Note data where ice shelf depth is >0 m results from regions where the ice shelf surface elevation is less than the firn correction. Points which plot below the 1:1 line are theoretically grounded. However, errors in the gravity derived topography with a standard deviation of ~100 m are noted (Fig. 4d), hence some areas which appear shallowly grounded may in fact be floating. In addition uncertainties in grounding-line position and real pinning points within the areas designated as ice shelves contribute to the observed scatter of anomalous points.

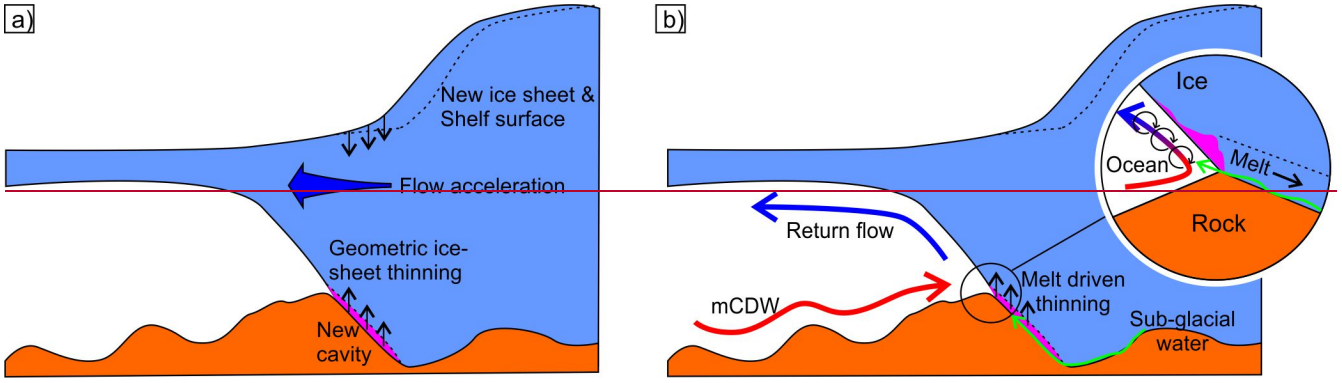

~~**Figure 6: Conceptual models of grounding line retreat. a) Geometric thinning. b) Enhanced grounding line melting.**~~

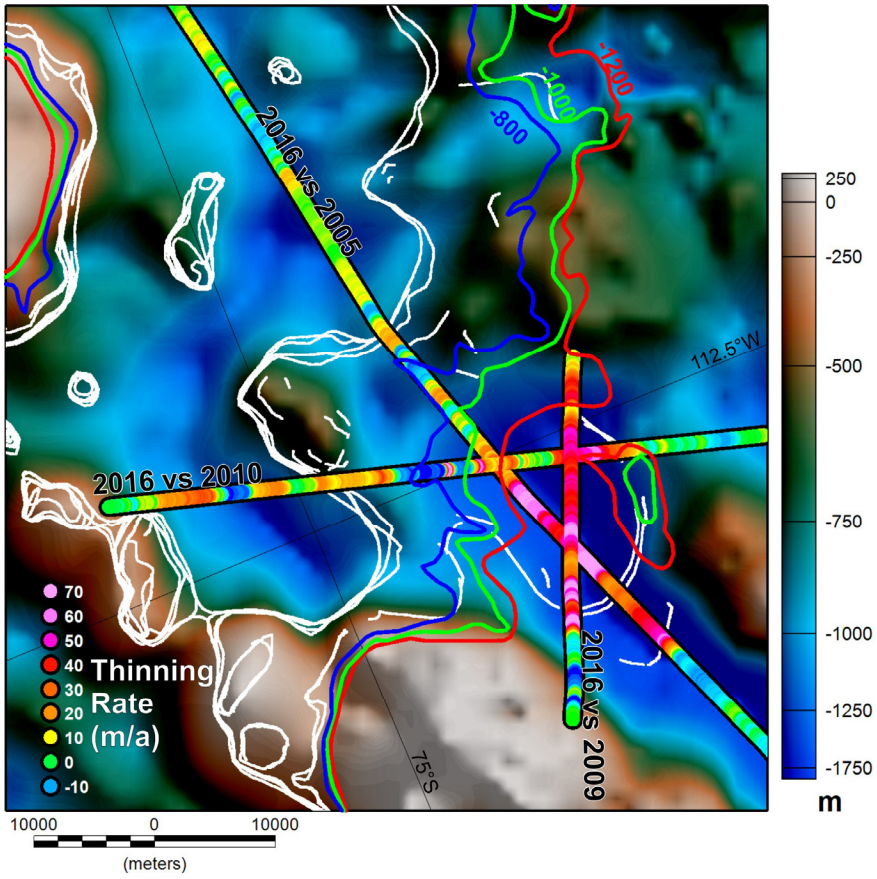

Figure ~~7~~6: Rate of Crosson Ice Shelf thinning determined by direct radio-echo sounding measurements from 2009, 2010, and 2016 OIB (Paden et al., 2010, updated 2018) and the 2005 AGASEA survey (Khazendar et al., 2016;Holt et al., 2006;Blankenship et al., 2012). Coloured contours show expected depth of base of floating ice shelf. White lines show INSAR derived grounding lines marking the front and back edges of the 'new' ice shelf (Rignot et al., 2014). For regional setting see Fig. 1d.

Supplementary material for: "New-gravity derived bathymetry for the Thwaites, Crosson and Dotson ice shelves reveals two ice shelf populations"

Tom A. Jordan[1], David Porter[2], Kirsty Tinto[2], Romain Millan[3], Atsuhiro Muto[4], Kelly Hogan[1], Robert D. Larter[1], Alastair G.C. Graham[5], John D. Paden[6]

[1] British Antarctic Survey, High Cross, Madingley Road, Cambridge, CB3 0ET, UK

[2] Lamont Doherty Earth Observatory

[3] Institut des Géosciences de l'Environnement, Université Grenoble Alpes, CNRS, 38000 Grenoble, France

[4] Dept. of Earth and Environmental Science, Temple University, Philadelphia, PA 19122, USA

[5] College of Marine Science, University of South Florida, St Petersburg, FL 33701, USA.

[6] Center for Remote Sensing of Ice Sheets (CReSIS), The University of Kansas, Kansas 66045, USA

Correspondence to: Tom A. Jordan (tomj@bas.ac.uk)

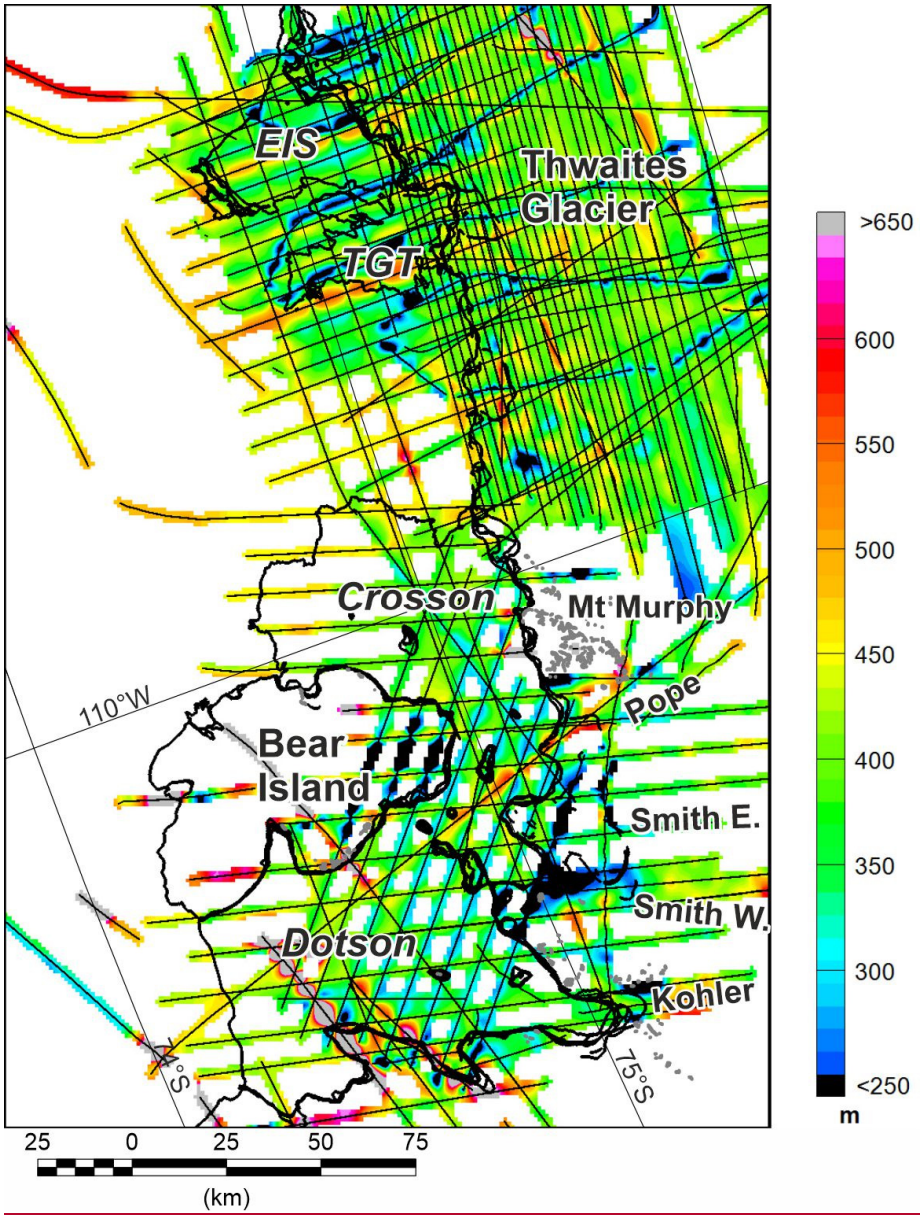

20 *SFig. 1. Range to ice surface for gravity flights used in this compilation (thin black lines). Note most flights cluster around 450 m ±200 m above the surface.*

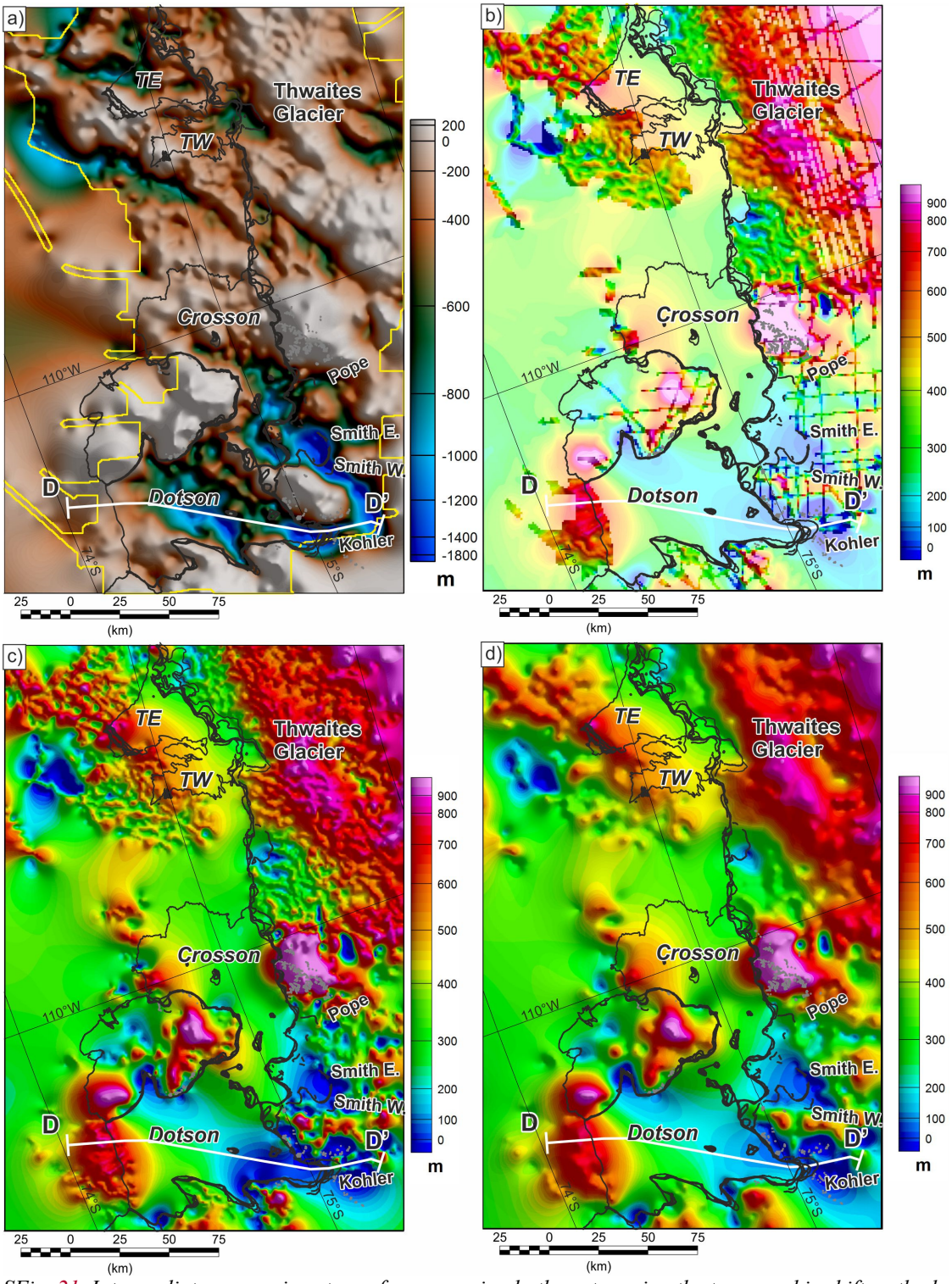

SFig. 21. Intermediate processing stages for recovering bathymetry using the topographic shift method. a) Initial equivalent topography recovered by iterative modelling of free-air gravity anomaly. Edge of free-air data in yellow. Profile D to D' shown in SFig. 43. b) Difference between observed topography (Main text Fig. 1d) and initial equivalent topography in (a) used in calculation of the final bathymetry. Strong colours show differences where both topographic observations and gravity data are present. Pale colours show interpolated difference field. c) Difference field interpolated with a tension of 0.25 and no pre-filter. d) Difference field interpolated with a tension of 0.25 after a 5km pre-filter of observed differences.

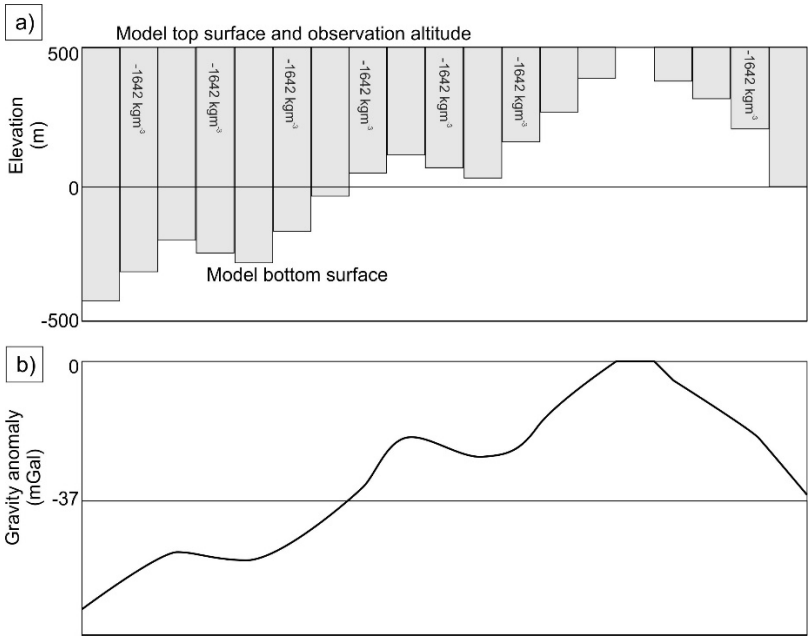

SFig. 3~~2~~. Sketch of gravity model setup and output. a) Structure of gravity model. The Gauss–Legendre quadrature (GLQ) method calculates the gravity effect of prisms of material. To efficiently calculate the gravity effect of a bathymetric surface (rock vs water) a series of prisms with this density contrast are therefore considered. b) Sketch of recovered gravity model. Note zero mGal where elevation is +500m.

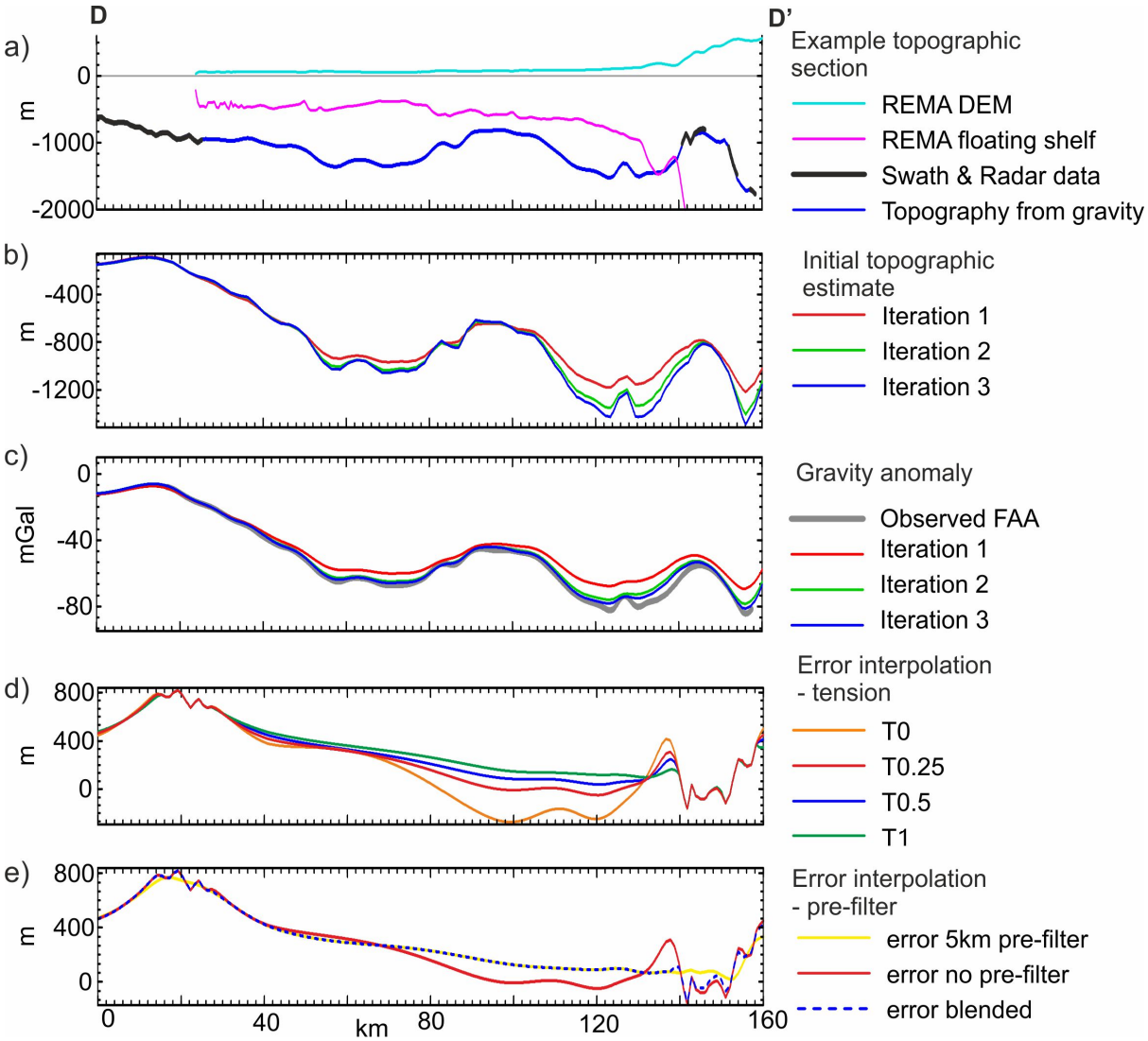

SFig. 43. Example cross section over Dotson Ice Shelf showing intermediate processing stages. See SFig. 21 for location. a) Output bathymetry, together with constraining swath and radar elevations. b) Initial topography during model iterations. Note Iteration 1 is the simple Bouguer slab conversion of the free air gravity anomaly to equivalent topography. c) Observed and modelled gravity anomalies with mean offset removed. Note rapid convergence along most of the profile. d) Impact of different interpolation tension factors (T0 to T1) on the interpolated error field. e) Impact of 5km pre-filter on interpolation of the error field, and final blended interpolated error filed used to correct initial topographic estimate.

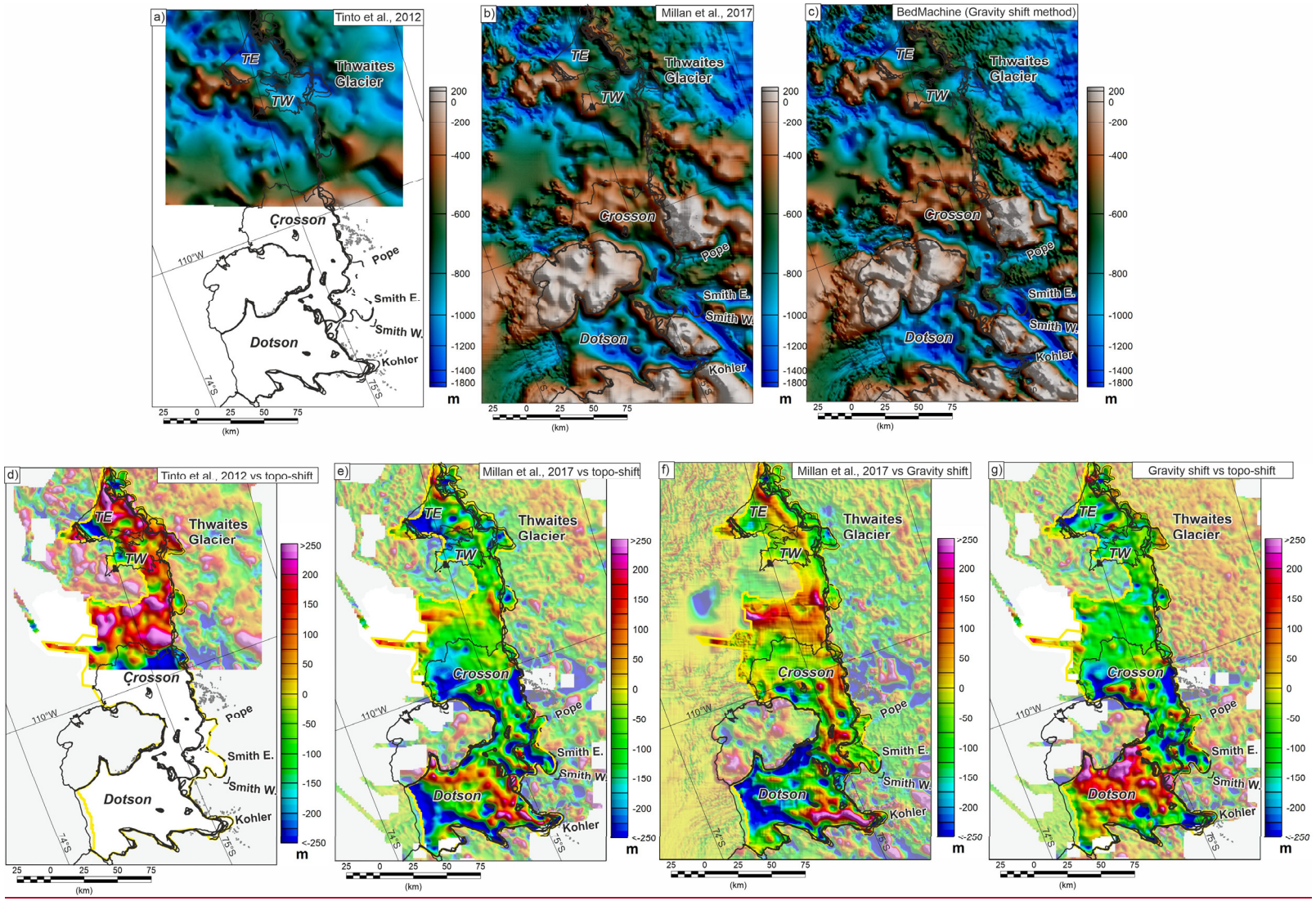

SFig. 54. Alternative gravity inversion results (a-c) and comparisons (d-g). Note errors in areas where data is constrained by other techniques are grey shaded. Differences in these areas do not reflect the differing gravity inversion methods, and are not discussed in this paper. a) Operation Ice Bridge (OIB) L3 V1 gravity to bathymetry inversion (Tinto et al., 2011). b) Millan et al., 2017 forward modelling result, tied to single coastal offset. c) BedMachine Antarctica (Morlighem et al., 2020) which used the "gravity shift method" (An et al., 2019). d) Comparison of topographic shift method with OIB result. e) Comparison of topographic shift method with Milan et al 2017. f) Comparison between BedMachine gravity shift method and Millan et al., (2017). g) Comparison of topographic shift and BedMachine implementation of the gravity shift method.

Section S1. Calculating sub-ice-shelf bathymetry using the topographic shift method

Step 1 – calculation of the initial bathymetric estimate

To calculate the sub-ice-shelf bathymetry the topographic shift method first calculates the "initial bathymetric estimate" by converting the free-air gravity anomalies to equivalent variation in topography (SFig. 21a). In the original implementation of the algorithm the Bouguer slab formula was used to directly calculate the initial bathymetric estimate (Hodgson et al., 2019). However, tests using a 3D model of the gravity anomaly associated with a 500 m deep, box shaped trough show that the Bouguer slab technique underestimates the topographic amplitude of narrower features, with errors of up to 10% for a modelled trough 10 km wide. We therefore applied an iterative forward modelling approach to recover a more accurate initial bathymetric estimate. For the gravity modelling we used a Gauss-Legendre Quadrature technique to model the gravity effect of a theoretical bathymetric surface (von Frese et al., 1981). This method calculates the gravity effect of a series of prisms on a 1 km x 1 km mesh (SFig. 32). An observation altitude of 500 m was assumed, and a density contrast of -1642 kgm^{-3} was imposed, equivalent to the contrast between water (1028 kgm^{-3}) and rock (2670 kgm^{-3}). These assumptions are valid as our study focuses on recovering sub-ice-shelf bathymetry, and the larger onshore ice versus rock density contrast is therefore neglected. The effect of the floating ice shelf is ignored as the gravity effect of the surface topography will be balanced by the effect of the low density keel to within the resolution of our data. The model assumptions led to a ~-37 mGal mean offset in the calculated gravity field which was removed before comparison with the observed data.

To initiate the gravity inversion (iteration 1), we converted the free-air anomaly to equivalent topography using the Bouguer slab formula (SFig. 43b). The gravity field was modelled (SFig. 43c) and the residual between observed and modelled gravity anomalies were calculated. The bathymetric surface was iteratively adjusted to reduce the calculated residual. An example profile shows how the topography changes with each iteration (SFig. 43b) and the convergence of modelled and observed gravity anomalies (SFig. 43c). It is apparent that the topographic iteration has not totally stabilised, but further iteration would over-fit the gravity data, potentially exaggerating the underlying bathymetry. After two stages of iteration the modelled and observed gravity field had converged to better than +/- 1 mGal across most of the survey area. Topography predicted to be above the observation surface was truncated, and the model did not converge in these regions.

Step 2 – correction to match observed topography

In the second stage, the algorithm corrects for differences between the initial bathymetric estimate (SFig. 21a) and topographic observations (Main text Fig. 1d). The calculated difference between the observed and initial bathymetric estimate reflects an integration of all geological factors, including long wavelength regional variations such as crustal thickness and more local factors such as sedimentary basins or intrusions (SFig. 21b). We assume that the calculated geologically-derived errors vary smoothly away from the constraining points and interpolate the difference field across the study area (SFig. 21b).

Creating and interpolating the difference field (SFig. 21b) is a critical step in calculating the sub-ice-shelf bathymetry. To estimate the difference field away from the control points we used tensioned spline

interpolation, as previously suggested for gridding both potential-field and bathymetric data (Smith and Wessel 1990). This technique has two end members, tension (T) = 0, equivalent to a minimum curvature fit to the data, and T=1, which provides an approximately linear interpolation between the control points (SFig. 43d). The minimum curvature approach is liable to generate extraneous oscillations away from control points, while a linear interpolation between the control points would be geologically unlikely. We therefore impose a tension factor of 0.25 which produces a result mid-way between the two end members (SFig. 43d).

Isolated short wavelength variations in topography at the edge of the control data-set can have a disproportionate impact on the interpolated difference field. This effect is mitigated by calculating the mean difference within a 5 km window before interpolation (SFig. 43e). In regions with control data a difference grid interpolated with no pre-filter was used (SFig. 21c), while away from the control data the interpolated difference grid after the 5 km pre-filter is used (SFig.21d). The transition between these two regions was blended using a weighted mean varying from zero to one over a 5km Gaussian smoothed transition zone around the observed data.

Section S2. International Thwaites Glacier Collaboration (ITGC) airborne gravity data processing.

Gravity data during the ITGC survey were collected on the BAS geophysically equipped twin otter using a strapdown gravity system (Jordan and Becker, 2018;Becker et al., 2015;Schwarz and Wei, 1990), and are available from the UK Polar Data Centre (Jordan et al., 2020). Average flight speed was ~60 ms^{-1}, and flights were flown draped, i.e. at an approximately constant terrain clearance, at 450 m. Raw acceleration data were recorded using an iMAR RQH-4001 inertial measurement unit (IMU) owned by Lamont- Doherty Earth Observatory. This sensor package, consists of three Honeywell QA2000 accelerometers (mounted in mutually perpendicular directions), and three ring laser gyroscopes. Coincident GPS data were recorded with a NovAtel receiver.

GPS and IMU data were ingested into the Terratec kinematic post processing software TerraPos and solved for a tightly coupled positional solution using a Precise Point Positioning (PPP) method. This included using precise ephemeris downloaded three months after data collection. The GPS antenna/INS lever arm was solved iteratively through three iterations of TerraPos and converged on: x=0.1881 y=0.3734 z=-1.5072 with variations at a sub cm level. Once the lever arm had been established this value was used for all subsequent flights, and the free-air gravity anomaly from the GRS80 ellipsoid was calculated at the same time as the position. Position, attitude and gravity data were then exported as 1Hz ASCII files which were imported into Geosoft Oasis Montage software suite for further analysis and levelling of the gravity data.

During the initial gravity processing Kalman filter parameters associated with the output gravity values were a 5km gravity correlation constant and a 10 mGal standard deviation. The stated performance of the iMAR IMU was also included in the Kalman filter. The correlation and standard deviation values were the system defaults in the TerraPos software and were used for all processing. Parameter tests of the impact of correlation and standard deviation were carried out and compared to Operation ICEBRIDGE (OIB) data (SFig. 65). These comparisons suggest the correlation factor has limited impact, but that it could in future be reduced to 2.5km. Increasing the

permitted standard deviation to 20 mGal gives a relatively noisy signal, while reducing the permitted standard deviation to 5 mGal gives an overly smooth solution.

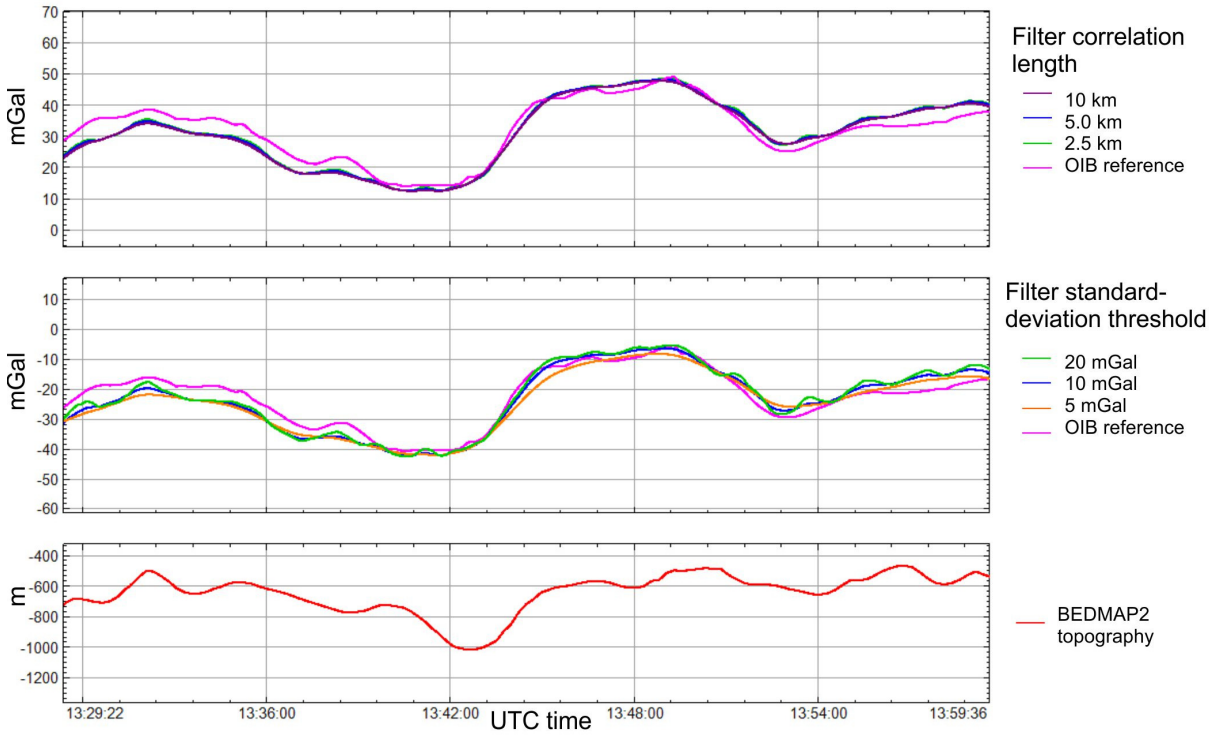

SFig. ~~5~~6. Impact of assumed correlation distance (top panel) and allowed gravity standard deviation (middle panel) on recovered free-air gravity values. For comparison OIB data gravity data collected on a coincident line are shown. Gravity outputs are not temperature corrected, but are all shown with the same amplitude vertical scale. Note the OIB data is sampled from a grid so artefacts due to cross lines may be present. Lower panel shows bed topography from BEDMAP2.

Overall the free air anomalies after initial processing show a clear geological/bathymetric pattern and correspond at short wavelengths to OIB data, but significant line to line noise is apparent (SFig. 7~~6~~ and 8~~7~~). To quantify this noise we compare our output free-air anomaly with gridded data from the OIB campaign in this region (SFig. 8~~7~~). There is a clear pattern across every flight with a shift of ~30mGal at the start of each flight, and a shift of ~60 mGal at the end.

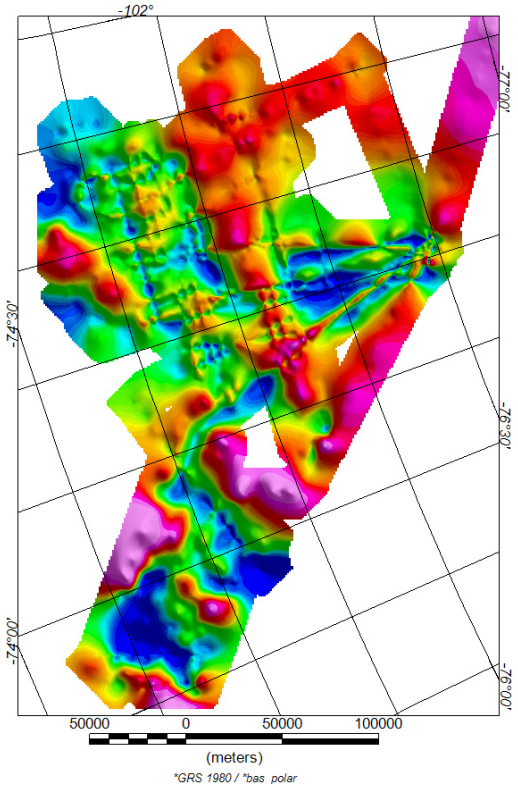

SFig. ~~6~~7. Map of initial free-air gravity anomalies prior to thermal correction.

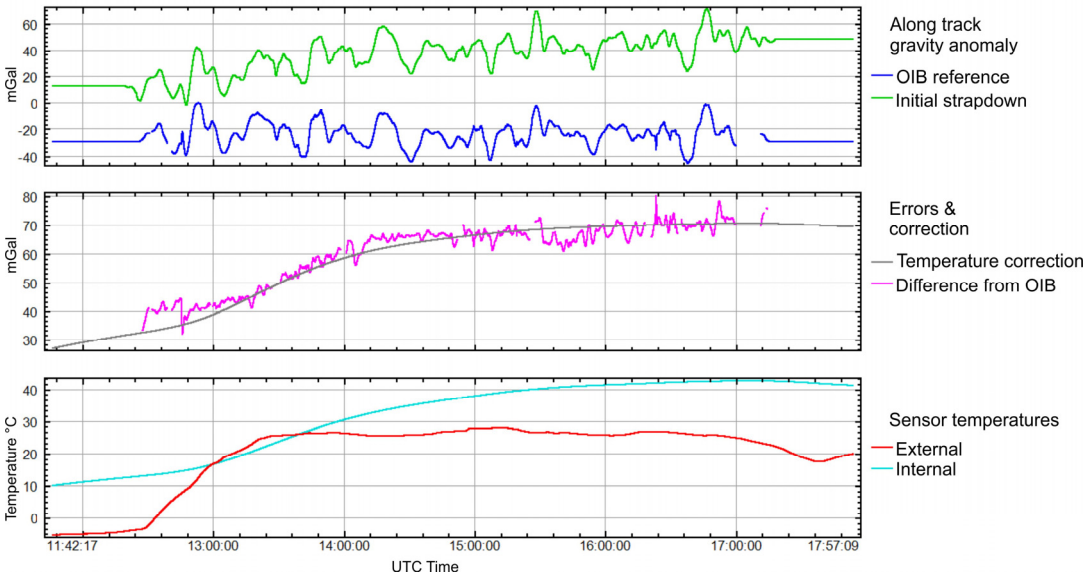

SFig. ~~7~~8. Example of initial processed free-air gravity anomaly along an entire flight, together with reference OIB data, and thermal effects and correction.

Plotting the internal sensor temperature reported for the IMU against the difference with OIB data confirmed that this error is dominantly a temperature effect (SFig. 9~~8~~). Generally the errors for all flights cluster along one path, but one flight has a systematic additional shift. The errors for this anomalous flight, together with errors far from the main cluster were discarded to get a better view of the temperature-induced error curve (SFig. 8~~7~~).

Taking these edited data points into Microsoft Excel and fitting a 2nd order polynomial provided ~~a good~~our model for the thermal drift:

Thermal error mGal = $-0.0174T^2 + 2.2619T + 5.8554$

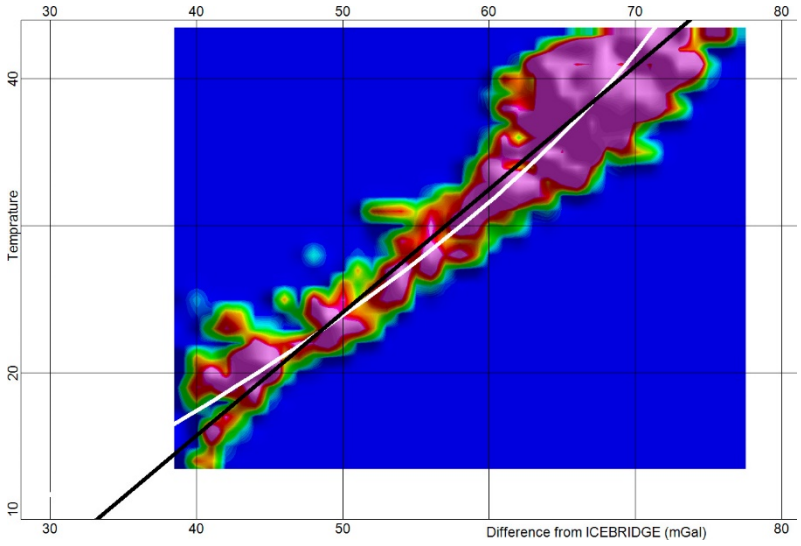

SFig. ~~8~~9. Temperature vs difference with OIB data density plot. Pink indicates many data points, blue indicates no data points. Note the data cluster is approximated by a straight line, with slope of 1.1934T (black). However, the 2nd order polynomial (white) tracks the error field more precisely.

After correcting for the overall thermal effects (SFig. 10~~9~~a) the crossover error was 7.09 mGal. Subsequent simple statistical levelling using a 3rd order trend fit to the crossover errors along each flight reduced the error to 2.84 mGal (SFig. 10~~9~~b). At this stage small residual errors with OIB on the order of +/- 3 mGal, with a wavelength of ~340 km (~2 hours) were evident. To remove this final error extreme errors, greater than +/- 8mGal, assumed to be gridding artefacts, were removed from the error values. A B-spline with smoothness of 1 and tension of zero (minimum curvature) was then fit to the residual error, and the resulting trend subtracted from the levelled free air anomaly. The final standard deviation of the crossover errors is 2.2 mGal, which equates to an error of 1.56 mGal.

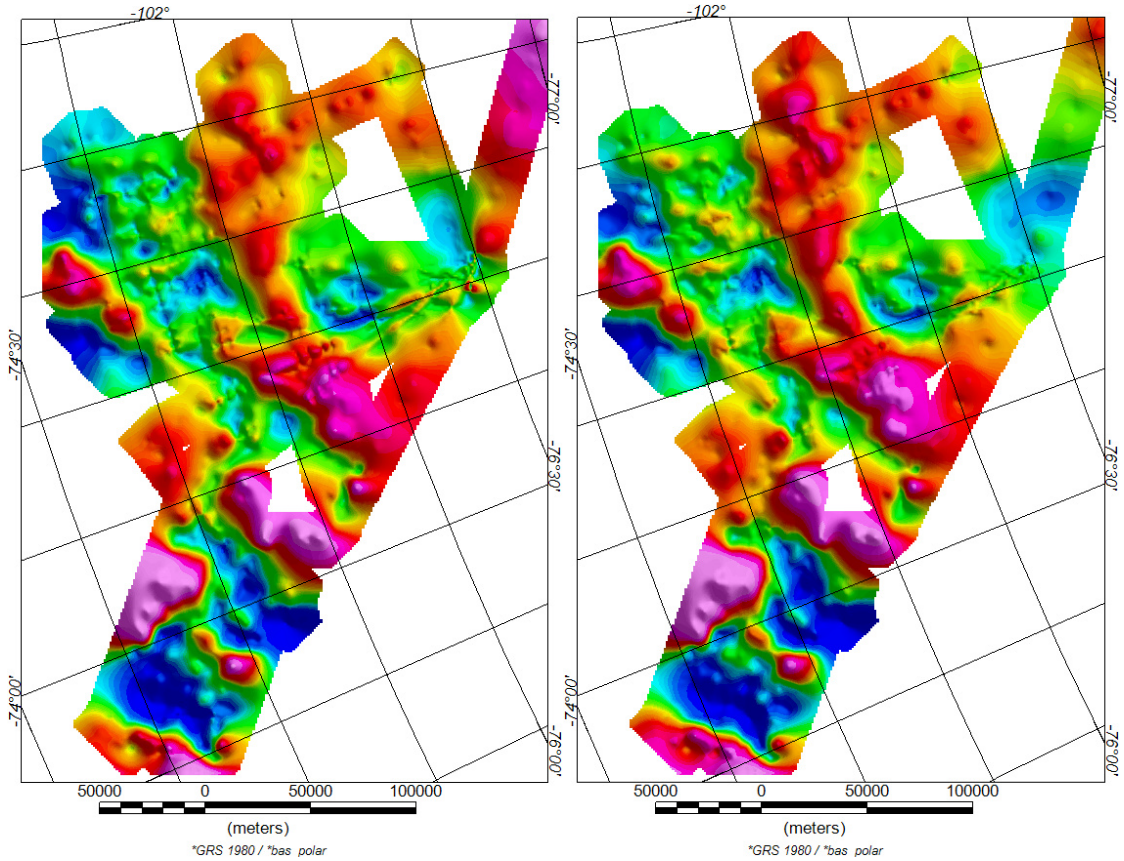

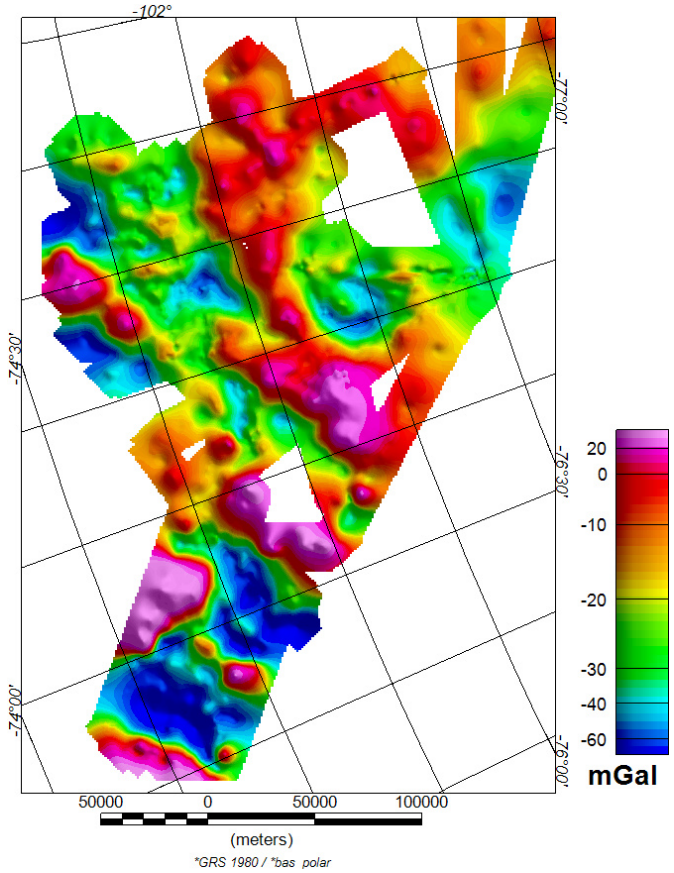

SFig. ~~9~~10. Free-air gravity anomalies. a) After initial thermal correction. b) After statistical levelling. c) Final gravity anomalies after along-line spline fit to the OIB dataset.

References

An, L., Rignot, E., Millan, R., Tinto, K., and Willis, J.: Bathymetry of Northwest Greenland Using "Ocean Melting Greenland" (OMG) High-Resolution Airborne Gravity and Other Data, Remote Sensing, 11, https://doi.org/10.3390/rs11020131 2019.

Becker, D., Nielsen, J. E., Ayres-Sampaio, D., Forsberg, R., Becker, M., and Bastos, L.: Drift reduction in strapdown airborne gravimetry using a simple thermal correction, Journal of Geodesy, 89, 1133-1144, 2015.

Hodgson, D. A., Jordan, T. A., De Rydt, J., Fretwell, P. T., Seddon, S. A., Becker, D., Hogan, K. A., Smith, A. M., and Vaughan, D. G.: Past and future dynamics of the Brunt Ice Shelf from seabed bathymetry and ice shelf geometry, The Cryosphere, 13, 545-556, 10.5194/tc-13-545-2019, 2019.

Jordan, T. A., and Becker, D.: Investigating the distribution of magmatism at the onset of Gondwana breakup with novel strapdown gravity and aeromagnetic data, Physics of the Earth and Planetary Interiors, 282, 77-88, https://doi.org/10.1016/j.pepi.2018.1007.1007, 2018.

Jordan, T. A., Robinson, C., Porter, D., Locke, C., and Tinto, K.: Processed line aerogravity data over the Thwaites Glacier region (2018/19 season). Natural Environment Research Council, UK Research & Innovation, UK Polar Data Centre, 2020.

Morlighem, M., Rignot, E., Binder, T., Blankenship, D., Drews, R., Eagles, G., Eisen, O., Ferraccioli, F., Forsberg, R., Fretwell, P., Goel, V., Greenbaum, J. S., Gudmundsson, H., Guo, J., Helm, V., Hofstede, C., Howat, I., Humbert, A., Jokat, W., Karlsson, N. B., Lee, W. S., Matsuoka, K., Millan, R., Mouginot, J., Paden, J., Pattyn, F., Roberts, J., Rosier, S., Ruppel, A., Seroussi, H., Smith, E. C., Steinhage, D., Sun, B., Broeke, M. R. v. d., Ommen, T. D. v., Wessem, M. v., and Young, D. A.: Deep glacial troughs and stabilizing ridges unveiled beneath the margins of the Antarctic ice sheet, Nature Geoscience, 13, 132-137, 10.1038/s41561-019-0510-8, 2020.

Schwarz, K. P., and Wei, M.: A framework for modelling kinematic measurements in gravity field applications, Journal of Geodesy, 64, 331-346, 10.1007/BF02538407, 1990.

Tinto, K., Bell, R. E., and Cochran, J. R.: IceBridge Sander AIRGrav L3 Bathymetry, Version 1., NASA National Snow and Ice Data Center Distributed Active Archive Center., Boulder, Colorado USA., 2011.

von Frese, R. R. B., Hinze, W. J., Braile, L. W., and Luca, A. J.: Spherical earth gravity and magnetic anomaly modeling by Gauss- Legendre quadrature integration, Journal of Geophysics, 49, 234-242, 1981.